



U.S. Department
of Transportation

Federal Railroad
Administration

Data Analysis Results of 70 Ton Boxcar Vibration Tests

Office of Research and
Development
Washington, D.C. 20590

George Kachadourian

Transportation & Telecommunications Engineering
The MITRE Corporation, Metrek Division
1820 Dolley Madison Boulevard
McLean, Virginia 22102

DOT/FRA/ORD-83/06

March 1983

This document is available to the
U.S. public through the National
Technical Information Service,
Springfield, Virginia 22161.

03 - Rail Vehicles &
Components

This document was disseminated under the sponsorship of the U.S. Department of Transportation in the interest of information exchange. The United States Government assumes no liability for its contents or use thereof. The United States Government does not endorse products or manufacturers. Trade or manufacturer's names appear herein solely because they are considered essential to the object of this report.

1. Report No. DOT/FRA/ORD-83/06	2. Government Accession No.	3. Recipient's Catalog No.	
4. Title and Subtitle RESULTS OF ANALYSIS OF 70 TON BOXCAR VIBRATION TESTS		5. Report Date March 1983	6. Performing Organization Code
7. Author(s) GEORGE KACHADOURIAN		8. Performing Organization Report No. MTR-82W00104	
9. Performing Organization Name and Address The MITRE Corporation/Metrek Division 1820 Dolley Madison Boulevard McLean, Virginia 22102		10. Work Unit No. (TRAI5)	11. Contract or Grant No. DTFR53-82-C-0087
12. Sponsoring Agency Name and Address The Federal Railroad Administration Office of Research and Development 400 Seventh Street, S.W. Washington, DC 20590		13. Type of Report and Period Covered Technical Report	
15. Supplementary Notes Project 1926A			
16. Abstract <p>This is the second of three volumes covering tests performed in April and May of 1981 at the Transportation Test Center (TTC) in Pueblo, Colorado on a 70 ton boxcar with Barber S-2-C trucks. The objective of the testing was to define the dynamic properties of the freight car for use in validating a mathematical model. The testing was conducted in two phases: (1) static tests were performed on each truck to characterize its stiffness and damping properties; (2) vibration tests were performed on the complete boxcar, loaded and empty, to determine resonant frequencies. Final results of Phase 1 have been documented in FRA/ORD-82/23 "Summary Results of 70 Ton Boxcar Testing", prepared by MITRE in April 1982. Results of the Phase 2 testing are covered in this report. This report defines the roll, bounce, pitch and yaw vibration characteristics of the boxcar; it also defines the carbody torsion and bending frequencies and resonant frequencies of the lading and presents comparisons between test results and the boxcar model to be validated. Results of the validation of the boxcar version of the computer program FRATE will be contained in FRA/ORD-(to be issued), "Validation of FRATE for Boxcars", the third and final report of the series.</p>			
17. Key Words Boxcar Vibration Testing Boxcar Dynamics Lading Dynamics Freight Car Truck Data		18. Distribution Statement Available to the Public through the National Technical Information Service, Springfield, Virginia 22161.	
19. Security Classif. (of this report) Unclassified	20. Security Classif. (of this page) Unclassified	21. No. of Pages	22. Price

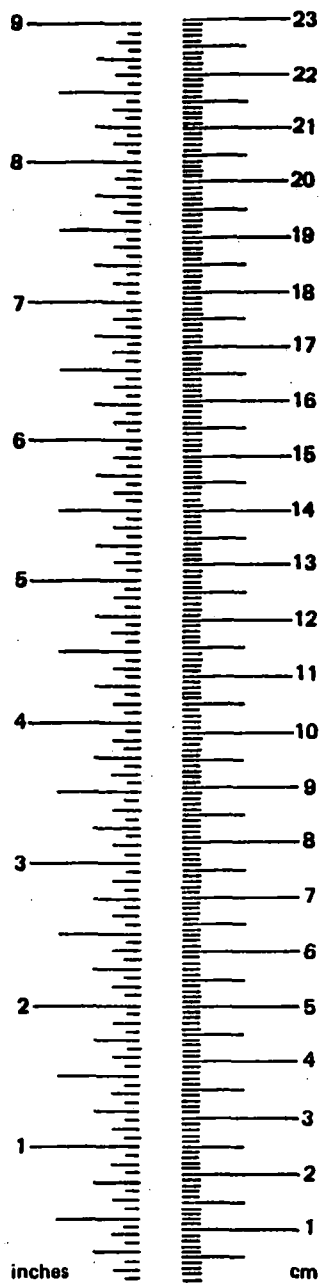
METRIC CONVERSION FACTORS

Approximate Conversions to Metric Measures

Symbol	When You Know	Multiply by	To Find	Symbol
LENGTH				
in	inches	*2.5	centimeters	cm
ft	feet	30	centimeters	cm
yd	yards	0.9	meters	m
mi	miles	1.6	kilometers	km
AREA				
in ²	square inches	6.5	square centimeters	cm ²
ft ²	square feet	0.09	square meters	m ²
yd ²	square yards	0.8	square meters	m ²
mi ²	square miles	2.6	square kilometers	km ²
	acres	0.4	hectares	ha
MASS (weight)				
oz	ounces	28	grams	g
lb	pounds	0.45	kilograms	kg
	short tons (2000 lb)	0.9	tonnes	t
VOLUME				
tsp	teaspoons	5	milliliters	ml
Tbsp	tablespoons	15	milliliters	ml
fl oz	fluid ounces	30	milliliters	ml
c	cups	0.24	liters	l
pt	pints	0.47	liters	l
qt	quarts	0.95	liters	l
gal	gallons	3.8	liters	l
ft ³	cubic feet	0.03	cubic meters	m ³
yd ³	cubic yards	0.76	cubic meters	m ³
TEMPERATURE (exact)				
°F	Fahrenheit temperature	5/9 (after subtracting 32)	Celsius temperature	°C

Approximate Conversions from Metric Measures

Symbol	When You Know	Multiply by	To Find	Symbol
LENGTH				
mm	millimeters	0.04	inches	in
cm	centimeters	0.4	inches	in
m	meters	3.3	feet	ft
m	meters	1.1	yards	yd
km	kilometers	0.6	miles	mi
AREA				
cm ²	square centimeters	0.16	square inches	in ²
m ²	square meters	1.2	square yards	yd ²
km ²	square kilometers	0.4	square miles	mi ²
ha	hectares (10,000 m ²)	2.5	acres	
MASS (weight)				
g	grams	0.035	ounces	oz
kg	kilograms	2.2	pounds	lb
t	tonnes (1000 kg)	1.1	short tons	
VOLUME				
ml	milliliters	0.03	fluid ounces	fl oz
l	liters	2.1	pints	pt
l	liters	1.06	quarts	qt
l	liters	0.26	gallons	gal
m ³	cubic meters	36	cubic feet	ft ³
m ³	cubic meters	1.3	cubic yards	yd ³
TEMPERATURE (exact)				
°C	Celsius temperature	9/5 (then add 32)	Fahrenheit temperature	°F



*1 in. = 2.54 cm (exactly). For other exact conversions and more detail tables see NBS Misc. Publ. 286, Units of Weight and Measures. Price \$2.25 SD Catalog No. C13 10 286.

RESULTS OF ANALYSIS OF 70 TON BOXCAR
VIBRATION TESTS

TABLE OF CONTENTS

	Page
LIST OF ILLUSTRATIONS	iv
LIST OF TABLES	vii
ACKNOWLEDGMENT	ix
EXECUTIVE SUMMARY	xi
1. INTRODUCTION	1
2. PROGRAM OBJECTIVES	1
3. TEST CONFIGURATIONS	2
4. GENERAL PROCEDURE FOR TESTING	7
5. DATA PROCESSING PROCEDURES	9
6. RESULTS OF DATA ANALYSIS	10
6.1 First Roll Mode	10
6.2 Second Roll Mode	12
6.3 Yaw Mode	15
6.4 Bounce Mode	17
6.5 Pitch Mode	19
6.6 Body Torsion Mode	20
6.7 Body Bending Mode	21
6.8 Lading Modes	22
6.8.1 Lading Lateral Mode	22
6.8.2 Lading Vertical Mode	25
6.9 Response to Staggered Rail Simulation	30
6.10 Hunting Simulation	36
6.11 Response to Vertical Bump Simulation	40
7. SUMMARY DISCUSSIONS	45
7.1 Modal Test Results	45
7.2 Track Condition Simulation	47
8. CONCLUSION	48
REFERENCES	49
APPENDIX A Measurements Numbering and Location	51

LIST OF ILLUSTRATIONS

<u>Figure No.</u>		<u>Page</u>
3.1	The DOTX 503 Boxcar on the Vibration Test Unit	2
3.2	Lading on Pallet Configurations	3
3.3	Arrangement of Lading in Boxcar	4
3.4	Corrugated Box Lading in Boxcar	4
3.5	Input Accelerometers Mounted on Boxcar Wheel	6
3.6	Accelerometer Block in Corrugated Paper Package	6
3.7	Accelerometer Block in Stretch Wrap Package	7
4.1	Vibration Test Unit Control System	8
6.1	Carbody Roll Motion in First Roll Mode	10
6.2	Summary Plot of First Roll Mode Frequencies	11
6.3	Summary Plot of Second Roll Mode Frequencies	13
6.4	Carbody Roll Motion in Second Roll Mode, Configuration 1B	13
6.5	Carbody Roll Motion in Second Roll Mode, Configuration 2	14
6.6	Carbody Roll Motion in Second Roll Mode, Configuration 3	14
6.7	Carbody Yaw Mode Frequency Summary	15
6.8	Relative Lateral Motion in Yaw Mode, Configuration 1B	15
6.9	Yaw Mode Shape, Configuration 1B	16
6.10	Bounce Test Responses, Configurations 1A & 1B	17
6.11	Bounce Test Responses, Configuration 3	18
6.12	Bounce Mode Frequency Variations	18
6.13	Pitch Frequency Variations	19
6.14	Body Torsion Mode Deflection Shape Configuration 1A, 12.72 Hz	20
6.15	Body Torsion Mode Deflection Shape Configuration 1B, 15.36 Hz	20
6.16	Carbody Bending Mode Deflection Shapes	21
6.17	Frequency Summary, Lading Lateral Mode, Variation With Input	23
6.18	Frequency Summary, Lading Lateral Mode Variation with Response	23
6.19	Lading Lateral Mode Deflection Shape Configuration 1A, 0.05 Inch Input	24
6.20	Lading Lateral Mode Deflection Shape Configuration 1A, 0.15 Inch Input	24

LIST OF ILLUSTRATIONS (Continued)

<u>Figure No.</u>		<u>Page</u>
6.21	Lading Lateral Mode Deflection Shape Configuration 1B, 0.05 Inch Input	24
6.22	Lading Lateral Mode Deflection Shape Configuration 3, 0.05 Inch Input	24
6.23	Frequency Response, Lading Vertical Motion, Configuration 1A, B End	26
6.24	Frequency Response, Lading Vertical Motion, Configuration 1B, B End	26
6.25	Frequency Response, Lading Vertical Motion, Configuration 3, B End	27
6.26	Frequency Response, Lading Vertical Motion, Configuration 1A, A End	27
6.27	Frequency Response, Lading Vertical Motion, Configuration 1B, A End	28
6.28	Frequency Response, Lading Vertical Motion, Configuration 3, A End	28
6.29	Comparison of Lading Vertical Response With and Without Friction Snubbers	29
6.30	Staggered Rail Test, Shock Impulse at Wheel	30
6.31	Staggered Rail Test, Configuration 1A Effect of Input level	32
6.32	Staggered Rail Test, Configuration 1B, Effect of Input Level	32
6.33	Staggered Rail Test, Configuration 2, Effect of Input Level	33
6.34	Staggered Rail Test, Configuration 3, Effect of Input Level	33
6.35	Staggered Rail Test--Effects of Configuration With 0.10 Inch Rectified Sine Input	34
6.36	Staggered Rail Test--Effects of Configuration With 0.20 Inch Rectified Sine Input	34
6.37	Staggered Rail Test--Effects of Configuration With 0.30 Inch Rectified Sine Input	35
6.38	Hunting Simulation Test With 0.20 Inch ($\pm 0.047^\circ$) Yaw Input, Carbody and Lading Lateral Motions Compared	36
6.39	Hunting Simulation Test, Response to 0.40 Inch ($\pm 0.094^\circ$) Yaw Input, Carbody and Lading Lateral Motions Compared	37
6.40	Hunting Simulation Test, Response to 0.60 Inch (0.14°) Yaw Input, Carbody and Lading Lateral Motions Compared	37
6.41	Hunting Simulation, Comparison of Accelerations in Lading Packaging, Measurement No. 45X	38
6.42	Example Time Traces of Lading Accelerometers Showing Characteristic Waveform With and Without Bumping	39

LIST OF ILLUSTRATIONS (Concluded)

<u>Figure No.</u>		<u>Page</u>
6.43	Vertical Bump Simulation, Configuration 1B, Vertical Responses	41
6.44	Vertical Bump Simulation, Configuration 1B, Lateral Responses	41
6.45	Vertical Bump Simulation, Configuration 2	42
6.46	Vertical Bump Simulation, Configuration 3	43
7.1	Frequency Range of Each Mode for All Configurations	46
A.1	Measurement Location on Carbody and Lading-- 70 Ton Boxcar	54
A.2	Measurement Location on Actuators and Trucks-- 70 Ton Boxcar	55

LIST OF TABLES

<u>Table Number</u>		<u>Page</u>
ES-1	Modal Frequency Summary, 70 Ton Boxcar, Hertz	xiii
3-1	Boxcar Configuration Data	5
3-2	DOTX 503 Weight and CG Data	5
3-3	Boxcar Dimension Data	5
6-1	Frequency Summary--First Roll Mode	11
6-2	Frequency Summary--Second Roll Mode	13
6-3	Frequency Summary--Bounce Mode	16
6-4	Frequency Summary--Pitch Mode	19
6-5	Body Torsion Mode Frequencies	20
6-6	Lading Lateral Mode Response Data	22
6-7	Lading Vertical Resonance Summary	25
6-8	Response in Hunting Simulation	38
6-9	Track Irregularity Test Results--Configuration 3	44
7-1	Modal Frequency Summary, 70 Ton Boxcar, Hertz	45
A-1	Measurement Number and Description	51

ACKNOWLEDGMENT

The contents of this report are the results of The MITRE Corporation's contribution to a larger program sponsored by the Department of Transportation, Federal Railroad Administration (FRA) under the leadership of Claire L. Orth of the Office of Rail Safety Research. William R. Walters, Rail Dynamics Laboratory (RDL)/FRA, and Dan W. Inskeep, RDL/BSI (Boeing Services International, Inc.) were responsible for the conduct of the testing as Test Manager and Test Engineer respectively. Data processing and computerized data analyses were performed by Firdausi Irani and Nicholas Wilson of BSI. The canned food used for the test lading was supplied by the Quaker Oats Company of Cedar Rapids, Iowa, and was arranged for by Dr. James W. Goff of the School of Packaging, Michigan State University. Dr. Goff also directed the lading configuration and packaging changes.

EXECUTIVE SUMMARY

Introduction

This is the second of three volumes covering a series of tests performed in the second quarter of 1981 on the DOTX 503 boxcar at the Transportation Test Center (TTC), Pueblo, Colorado. The tests were performed by Rail Dynamics Laboratory (RDL) personnel and were sponsored by the Federal Railroad Administration (FRA), Office of Research and Development in their continuing study of the safety aspects of track-train dynamics. The MITRE Corporation role was to provide technical assistance to the FRA in planning, performance monitoring and results evaluation. The program was divided into the following three phases:

- The first, which has been completed, consisted of static tests performed on each truck of the DOTX 503 Boxcar: these results are presented in Reference 1.*
- The second phase, which is the subject of this report, consisted of vibration tests performed on the complete boxcar.
- The third phase will consist of validating the boxcar version of the computer program FRATE and will be reported in Reference 2.

Test Objectives

The primary objective of the test program was to develop a data source on the dynamic properties of freight cars in a form that could be used to validate the boxcar version of FRATE, a computer program for analyzing freight car dynamics. Broader objectives were to perform the FRATE validation and demonstrate a validation procedure. The end result would be an analysis tool capable of accurate, over-the-road freight car response calculations for use by the railroad industry.

Test Description

The vibration testing of the boxcar was performed on the Vibration Test Unit (VTU) located in the RDL. The VTU has a system of 12 hydraulic actuators, one placed under each wheel of the car acting vertically and one beside each axle acting laterally, with the weight of the car carried by the eight vertical actuators. A set of flat and spherical bearings at each truck permits independent motion of each actuator and enables the VTU to impose any combination of motions in five degrees of freedom. The actuators are controlled with a Varian V-73 digital computer.

Four configurations were tested.

- Configuration 1A was with 60 tons of canned food in corrugated paper boxes.
- Configuration 1B was the same as 1A but with friction snubbers removed.
- Configuration 2 was the empty boxcar with friction snubbers removed.
- Configuration 3 had the same 60 tons of canned food but in stretch wrap packaging and with friction snubbers.

Two general types of vibration tests were performed, modal and response. The modal tests input sinusoidal motions with frequency varied at a preset, logarithmic rate with the objective of identifying the resonant frequencies of the car and contents and measuring the deflection shapes at resonance. The frequency range and shaker phasing were varied depending on the particular mode being tested. The response testing consisted of simulating three track conditions and measuring the response of the carbody and lading.

*The list of References can be found at the end of the report.

The FRATE validation process will consist of an analytical performance of the test procedures and a comparison of analytical and test results.

Summary of Results

There were two significant difficulties encountered in the course of testing. One was due to the character of the friction snubbers: they were very stiff and very effective in subduing vehicle motion, and as a consequence not all modes were found in the "with snubber" configuration. The other difficulty encountered was in the computer programming and shaker motion control for the track irregularity tests. However, despite these gaps in the planned testing, because some redundancy was included in the test procedures all objectives were met and the testing was satisfactorily completed.

A summary of the modal frequencies obtained in each of the four configurations tested, and a set of FRATE analysis results, is given in Table ES-1. The best frequency agreement is seen to occur between the FRATE analysis with friction snubbers and test Configuration 1B (without friction snubbers). The only mode that is significantly different is the second roll mode. It was concluded that the friction snubber model in FRATE needs to be modified. Further it may be necessary to make a change to the truck suspension roll spring rates, presently tri-linear, to obtain improvement in the second roll mode without adversely affecting other modes. With these two changes and with stiffness changes indicated by the results of truck static tests, it is anticipated that validation of the boxcar version of FRATE will be accomplished with little difficulty.

The two lading package configurations tested were a corrugated fiberboard box and a plastic stretch wrap. The stretch wrap appeared to protect the cans in that they were held firmly together and did not rattle and slide as they did in the fiberboard box configuration. However, there was no significant difference seen in the overall responses of the two loadings. It was concluded that the pallet used and the height of the lading stack were the two factors that determined overall lading responses.

The lateral resonant mode of the lading fell in the 1.6 to 2.8 Hertz range, with the variation due to the effect of amplitude of motion. These frequencies are low enough to couple with and affect the carbody roll mode and have the equivalent effect of a boxcar with more weight and a higher center of gravity. The lading lateral mode also overlaps the carbody yaw mode and can have a detrimental effect on carbody hunting conditions since carbody yaw is the mode commonly involved in body hunting.

Alleviation of the adverse effects of the lateral lading mode can be obtained by the use of a more rigid pallet, by having minimum voids between lading stacks and by filling the voids with a durable dunnage.

TABLE ES-1 MODAL FREQUENCY SUMMARY, 70 TON BOXCAR, HERTZ

CONFIGURATION DATA MODE	PREDICTION 57.5 Ton Part Time Snubbers	CONFIG 1A 60.1 Ton Snubbers In	CONFIG 1B 60.1 Ton Snubbers Out	CONFIG 2 Empty Snubbers Out	CONFIG 3 59.5 Ton Snubbers In
1st Roll	0.7	.69-.98	.54-.69	.84-1.00	.65-1.2
2nd Roll	1.6	N.A.	2.5-3.0	3.04	3.40-4.0
Yaw	1.7	N.A.	1.65-1.71	2.3-2.6	N.A.
Bounce	2.2	N.A.	2.05	3.81	2.1-2.8
Pitch	2.9	3.4-4.5	2.77	4.34	3.3-4.4
Body Torsion	--	12.4 & 14.1	13.67 & 15.36	13.125 & 14.75	13.17& 14.8
Body Bending	--	Above 20.0	Above 20.0	Above 20.0	Above 20.0
Lading Lat.	3.0	1.7-2.8	1.65-1.71	--	1.60-2.4
Lading Vert.	9.0	8.5-8.7	9.00-9.25	--	8.25-8.5

NOTES:

N.A. - not available (snubbers remained locked)

Body Torsion - Two modes were found: (1) coupled with carbody yaw;
(2) uncoupled.

1. INTRODUCTION

This report contains the results of vibration tests performed on the DOTX 503 Boxcar, a 70-ton high cube with Barber S-2-C trucks, at the Transportation Test Center (TTC) in Pueblo, Colorado in May of 1981 under the sponsorship of the Federal Railroad Administration (FRA). The purpose of the testing was to obtain the dynamic response characteristics of the boxcar, including the effects of three configuration changes. The test results will be used in the validation of the boxcar version of FRATE (Freight Car Response Analysis and Test Evaluation), a computer program for analyzing freight car dynamics, as well as to provide information on boxcar dynamics for the railroad industry (suppliers and operators).

The test program is in three phases. The first consisted of static tests performed on each truck from the DOTX 503 Boxcar to determine its stiffness and damping properties under vertical, lateral, and roll load conditions. The results of these truck characterization tests have been reported in Reference 1.* The second phase consisted of vibration tests performed on the complete boxcar and is the subject of this report. The third phase will consist of the validation of the boxcar version of the computer program FRATE and will be reported in Reference 2. A test report by Wilson of Boeing Services International, Inc. (BSI) has also been issued (Reference 3) summarizing the testing of phases 1 and 2.

1.1 Background

Current trends in U.S. railroading are towards heavier freight cars, higher speeds, and more cost-effective maintenance of cars and way. Each of these trends puts the freight car closer to a critical edge of safety: loads are higher on both track and car; margins are reduced, both knowingly, for cost-saving purposes, and unknowingly, because track and car design are largely empirical; and wear rates and failure rates are increased.

Because of decreased margins, the dynamics of the freight car have become more important and in many cases have become the incremental difference between safe and unsafe operations. The car dynamics not only can cause or be a contributing cause to a derailment, but also can have caused wear or failure

in the component which caused derailment. With recognition of its increasing importance in the safe operation of railroads, there have been continuing experimental and theoretical efforts aimed at obtaining better definitions and understanding of freight car dynamics. The resulting increased knowledge and analysis capability is being used to aid the development of design changes and to quantify safety margins.

1.2 FRATE

One of the FRA's involvements in the area of track-train dynamics has been in the development and validation of FRATE (Freight Car Response Analysis and Test Evaluation). The program was initially set up for the analysis of trailer on flatcar (TOFC) and was validated for that configuration of freight car (Reference 4). The program has been expanded to include analysis of boxcars as well as TOFC and a user's manual covering both has been issued (Reference 5). The test results of this report will be used to validate the boxcar versions of FRATE.

FRATE is a digital computer program which solves a set of coupled nonlinear differential equations in the time domain. Solution is obtained using a Runge-Kutta numerical integration procedure--the analysis procedure being to input a force or motion and calculate the resulting response motions and forces. The trucks, carbody, and lading are modeled as lumped masses with interconnecting springs. The carbody flexibility is included through a normal mode representation.

2. PROGRAM OBJECTIVES

The primary objective of the test program was to develop a source of information on the dynamic properties of freight cars in a form that can be used to validate the boxcar version of the computer program FRATE. The dynamic properties of the test boxcar to be obtained were, (1) its modal characteristics and (2) its responses to simulated track condition. The influence that gross weight, friction snubbers, and amplitude of motion have on the boxcar dynamic properties were to be determined. Two types of packaging--corrugated boxes and a plastic stretch wrap--were also tested to evaluate their differences. The broader objectives of the program are to validate the boxcar version of the FRATE program and, in the process, demonstrate a validation procedure and

*The list of References can be found at the end of the report.

make available an analysis tool capable of accurate over-the-road boxcar response calculations.

The objectives of the modal testing were to identify resonant frequencies, to define the deflection shape at each resonance, to obtain a measure of the damping associated with each resonance, and to measure nonlinear effects with respect to amplitude of motion and configurational changes.

The term "modal" in correct usage implies a nearness to the orthogonality of normal modes. The freight car "modes" are for the most part damped, coupled and nonlinear and are more accurately termed as resonant conditions rather than modes. However, the terms "mode" and "modal" are used in this report as a matter of convenience with the understanding that "resonance" is the more correct term.

The objective of the response testing was to obtain a measure of responses on and in the boxcar to simulations of two track profile conditions and one hunting condition.

Comparison between test and FRATE analysis for both types of tests will indicate the accuracy of FRATE. How-

ever, the modal comparison will indicate causes of differences, whereas the response tests are a more direct measure of accuracy.

For the lading, in addition to the model validation objectives, the relative performance of two shipper designs were to be evaluated.

3. TEST CONFIGURATIONS

The vibration testing of the DOTX 503 Boxcar was performed with the boxcar mounted on the Vibration Test Unit (VTU) in the Rail Dynamics Laboratory (RDL). A photograph of the boxcar on the VTU is shown in Figure 3.1. Two safety restraint systems were used; one to limit roll motions and the other to restrict longitudinal motions. The roll limiting devices were located at four points, one on each side of the carbody opposite each truck. They each consisted of a linkage connected at the side of the boxcar and at the laboratory floor by spherical bearings. The length of the linkages could vary with sliding contact up to a $\pm 30^\circ$ limit of roll of the boxcar at which point the linkages would bottom against a set of Bellville springs. The longitudinal restraints acted through the buff and draft cushioning within the coupling

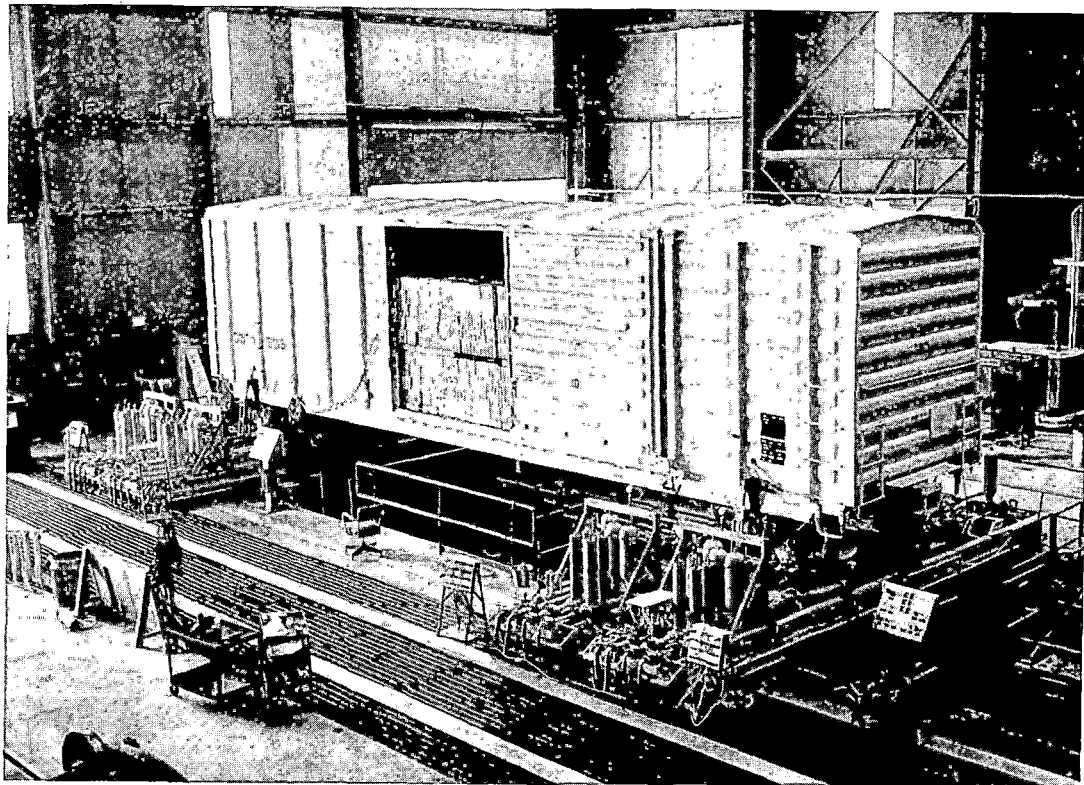


FIGURE 3.1 THE DOTX 503 BOXCAR ON THE VIBRATION TEST UNIT

gear with a longitudinal tension force of 20,000 pounds which is within the normal range of consist conditions.

The two lading configurations tested used the same canned food but in different packaging, a corrugated paper box and a stretch wrap package. Both lading configurations used wooden pallets and both were loaded in the boxcar two pallet stacks high, the lower pallet having four layers of lading packages and the upper pallet having five layers. The arrangement of lading on pallets is shown in Figure 3.2. and the arrangement of the pallets in the boxcar is shown in Figure 3.3. The photograph in Figure 3.4 shows the corrugated box configuration partially loaded in the boxcar.

Testing was performed in the four configurations shown in Table 3-1. A break down of the weight components and center of gravity (c.g.) height is given in Table 3-2. The difference in weight between the two ladings is due to the heavier weight of the corrugated paper boxes. Boxcar dimensional data is given in Table 3-3.

Measurements of inputs to and responses of the test vehicle were made with Endevco Model 2262-25M15, + 25g, Piezoresistive Accelerometers. Accelerometer numbering systems and location descriptions are given in Appendix A. Other measurements consisted of Trans-

Tek displacement transducers Models 245-000 and 246-000 and two gyros to determine carbody roll angles. Video cameras were used to monitor and record visible motions of the car and lading.

The accelerometers used to measure inputs to the boxcar were bonded to the car wheels with an interfacing mounting block contoured to fit the wheel as shown in the photograph of Figure 3.5. It should be noted that shaker control was with displacement transducers built into the shaker heads while the "input" accelerometers were used in the analysis.

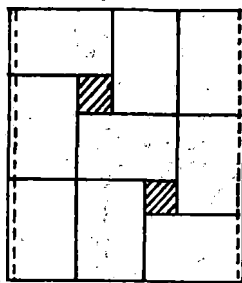
The accelerometers used to measure lading response were mounted in blocks of wood with the same dimensions as the canned food. The blocks were made rectangular instead of cylindrical to provide a more accurate orientation of the accelerometers. An instrumented block of wood took the place of one can in each instrumented lading package. Example installations are shown in the photograph of Figures 3.6 and 3.7.

The instrumentation used in the analysis of test results is described in Appendix A.

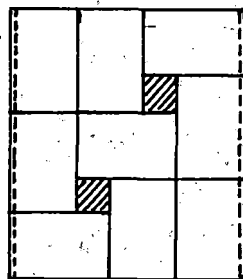
CORRUGATED PAPER PACKAGE

Package Size = 18 x 12 x 9 inches

9 packages per layer, 48 x 42 inch footprint



pattern A

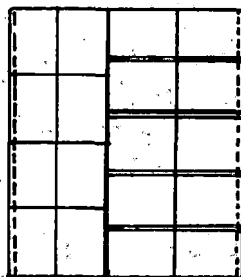


pattern B

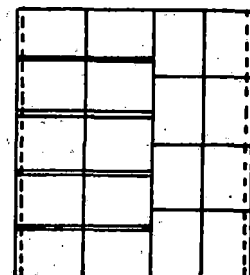
STRETCH WRAP PACKAGE

Package size = 12 x 9 x 8 1/8 inches

18 packages per layer, 48 x 42 inch footprint



pattern A

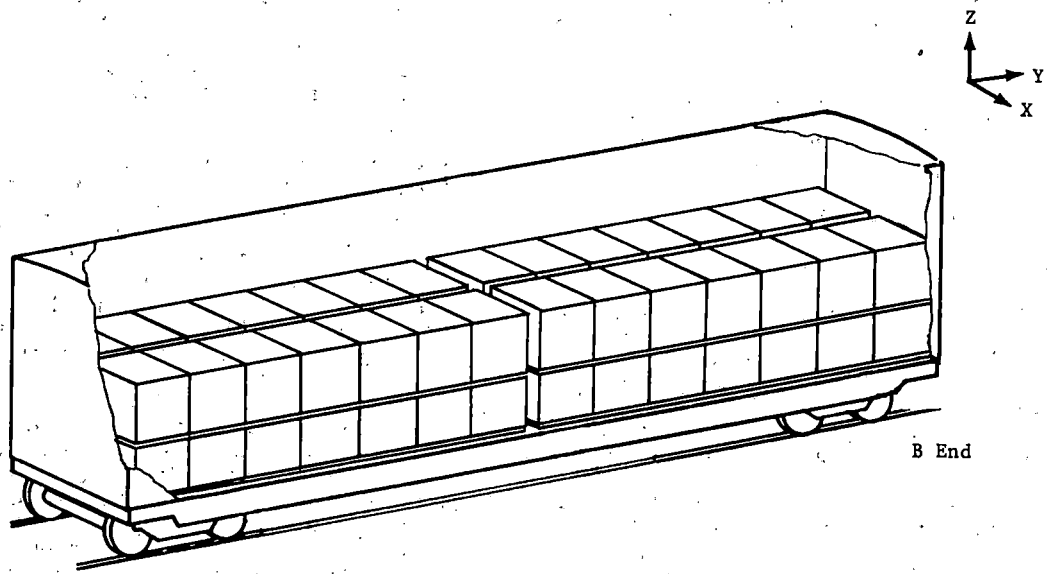


pattern B

Pallet surface = 48 x 40 inches

Lading arranged in alternating layers of patterns A and B.

FIGURE 3.2 LADING ON PALLET CONFIGURATIONS



A End

B End

Top Pallets have 5 Layers of Packaged Lading
 Bottom Pallets have 4 Layers of Packaged Lading

FIGURE 3.3 ARRANGEMENT OF LADING IN BOXCAR

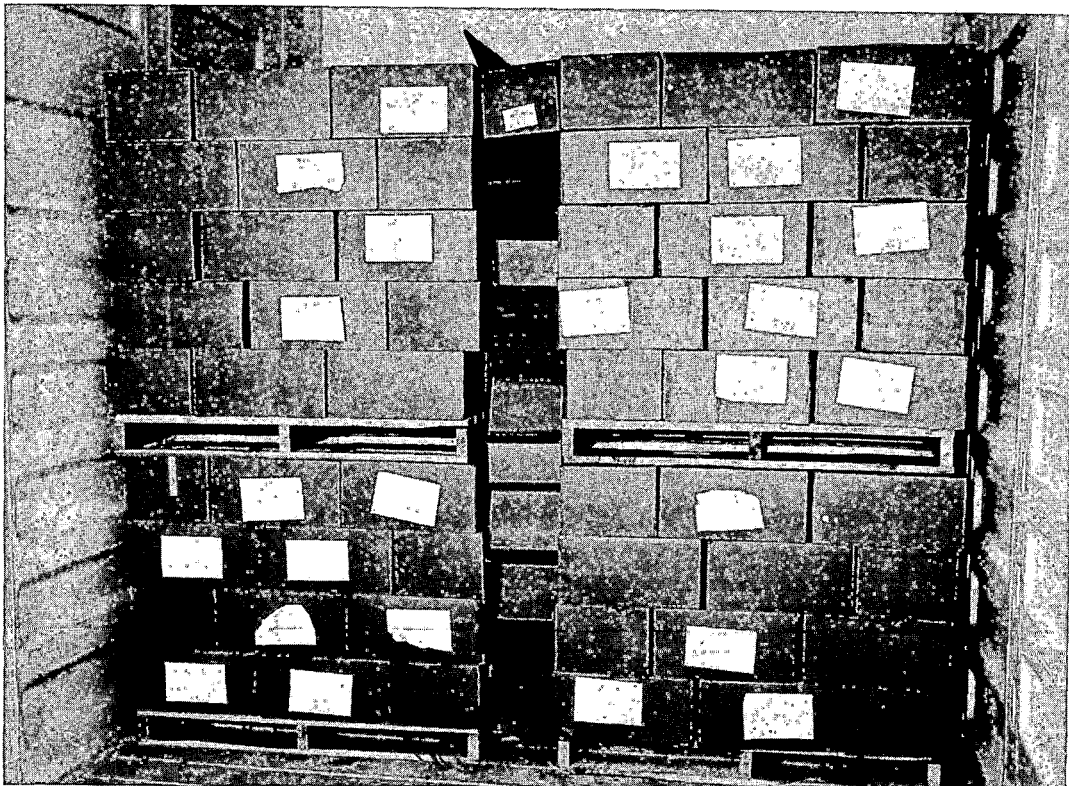


FIGURE 3.4 CORRUGATED BOX LADING IN BOXCAR

TABLE 3-1 BOXCAR CONFIGURATION DATA

Configuration Number	Lading Package	Gross Weight (lbs.)	Snubbers
1A	Paper Box	181700	Active
1B	Paper Box	181700	Removed
2	Empty Car	61600	Removed
3	Stretch Wrap	180569	Active

TABLE 3-2 DOTX 503 WEIGHT AND CG DATA

Item	Weight (lb.)	CG Height (in.)	W x h (10 ⁶ lb. in)
Trucks (both)	17400	16.5	.2871
Carbody	44200	67.37	2.9777
Lading (1)	120100	86.0	10.3286
Lading (2)	118960	82.0	9.7547
Carbody & Lading (1)	164300	81.0	13.3063
Carbody & Lading (2)	163160	78.0	12.7324

- (1) Corrugated paper box packaging
- (2) Plastic stretch wrap packaging

TABLE 3-3 BOXCAR DIMENSION DATA

Item	Value
Inside Length	50 Feet
Inside Width	9 Feet
Inside Height	11 Feet
Volume	5300 Cubic Feet
Truck Spacing	40 Feet, 10 Inch
Height of Car Floor	43.5 Inches Above Top of Rail
C.G. Height (Empty)	53 Inches Above Top of Rail

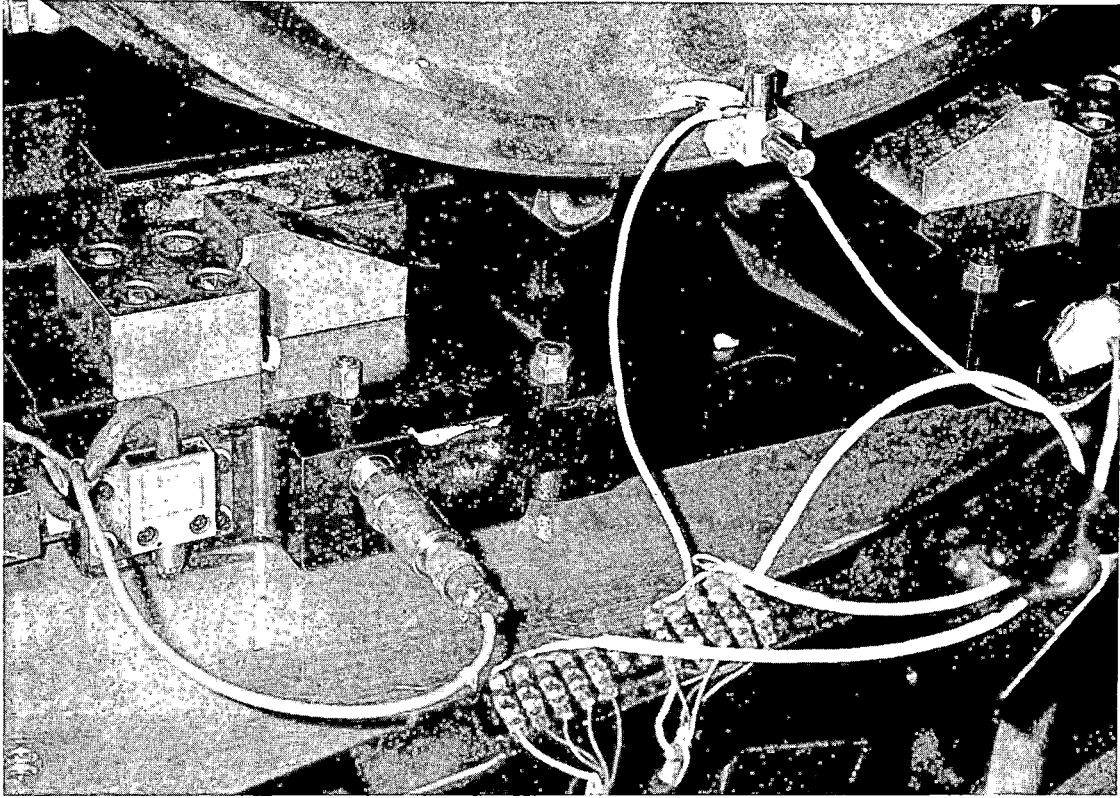


FIGURE 3.5 INPUT ACCELEROMETERS MOUNTED ON BOXCAR WHEEL

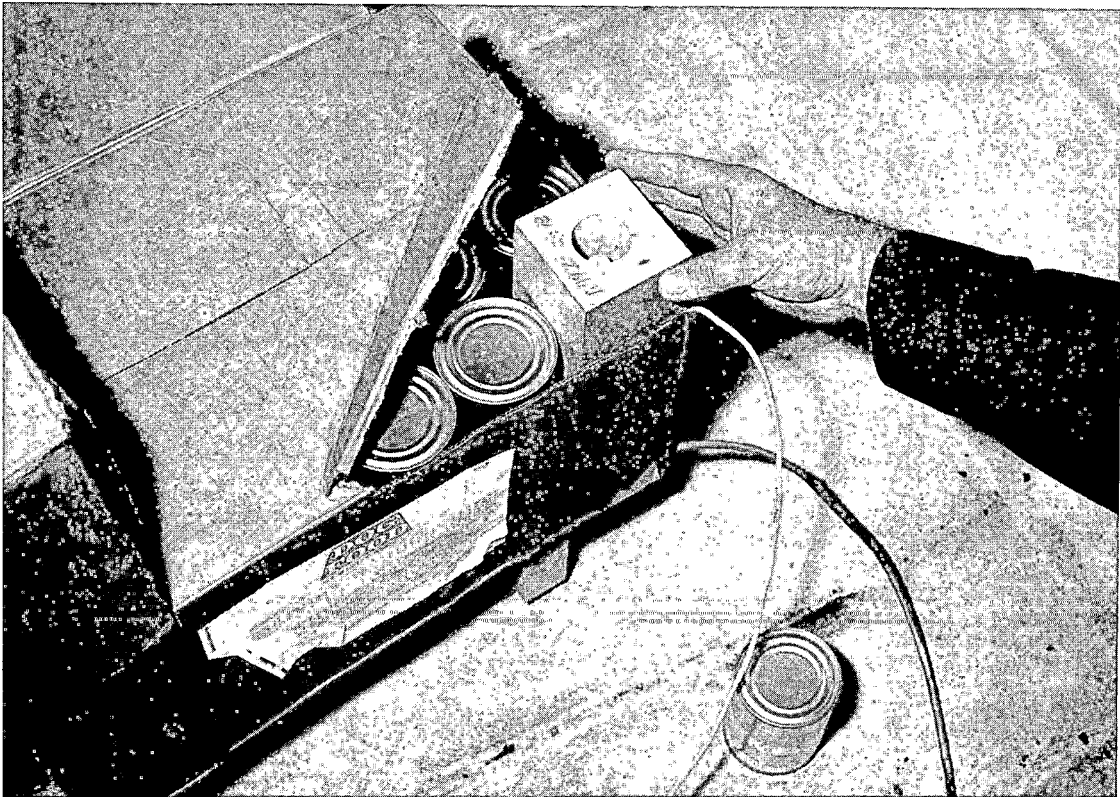


FIGURE 3.6 ACCELEROMETER BLOCK IN CORRUGATED PAPER PACKAGE

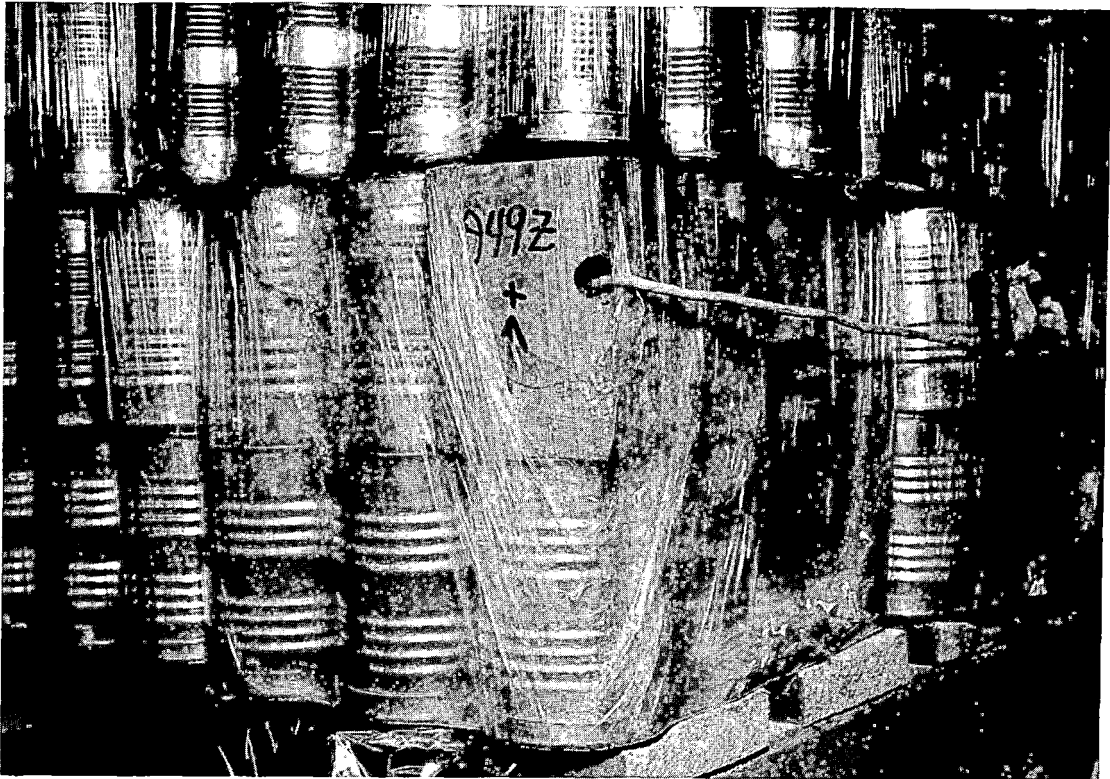


FIGURE 3.7 ACCELEROMETER BLOCK IN STRETCH WRAP PACKAGE

4. GENERAL PROCEDURE FOR TESTING

The VTU imposes motions at the test vehicle wheels with 12 hydraulic actuators: one under each wheel to input vertical motion and one beside each axle to input lateral motion. The three actuators at each axle are interconnected through a bearing assembly that enables each actuator to move independently of the other. With this arrangement the VTU is able to impose any combination of motions in five degrees of freedom (vertical, lateral, roll, yaw and pitch) as well as reproduce a measured or simulated track geometry.

A simplified block diagram of the VTU Control System is shown in Figure 4.1. The shaker system is controlled using a Varian V-73 Computer (the ICSN in Figure 4.1). The motions to be generated in a test run are defined in a Run Information File (RIF). The RIF is input to the computer which then controls the hydraulic actuators in a servo loop using a displacement transducer built into each actuator. Response measurements can also be monitored by the ICSN system and the test automatically stops when preset limits are exceeded.

Quick look data read-out are made as shown in Figure 4.1 using analog signals.

Recording for final data analysis is made, after analog to digital (A/D) conversion, on magnetic tape.

Modal testing was performed by applying sinusoidal motions at the wheels with the frequency of input varied at a prescribed rate through a frequency range encompassing the predicted resonant frequency. The shaker configurations, that is the relative phase and amplitude of the twelve actuators, were adjusted for each mode to be in synergy with the expected deflection shape of that mode. The general procedure followed was to perform a frequency sweep and to review oscillograph records and Brush Recorder Charts to evaluate the test results. A decision would then be made whether to continue to the next test or to repeat the test run with possible variation of the test procedures.

The track condition tests were run with much the same procedures as the modal tests with the RIF containing a definition of wheel-rail interface motions simulating the particular track condition. The test procedures defined in References 6 and 7 were followed in detail. A log of the test runs made is given in Reference 1. The test report of Reference 3 includes further details of the test configurations and measurements.

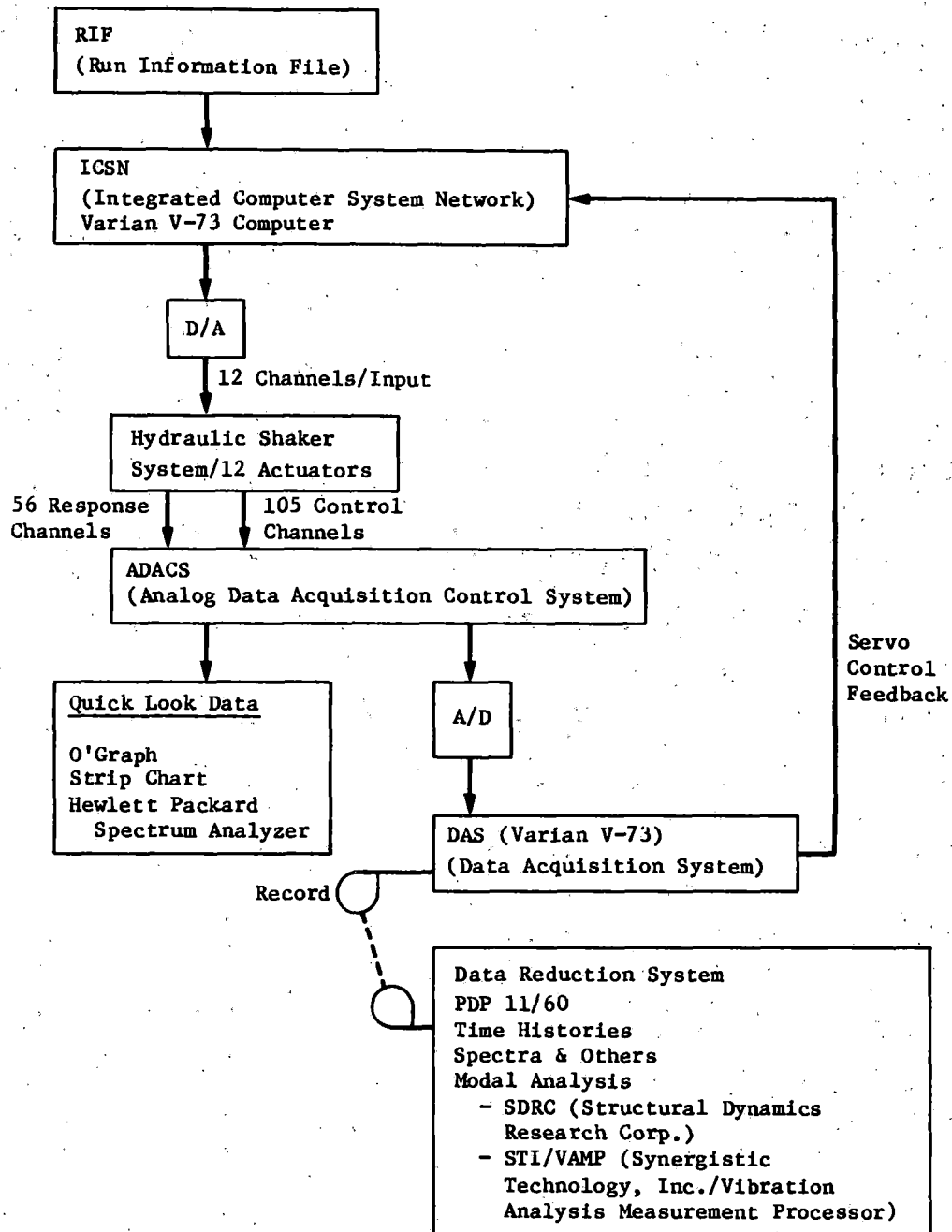


FIGURE 4.1 VIBRATION TEST UNIT CONTROL SYSTEM

5. DATA PROCESSING PROCEDURE

Objectives of the data processing for the two types of tests (modal and response) were as follows:

- (1) Modal Testing
 - identify modes (resonant frequencies)
 - measure modal damping
 - measure modal shapes
 - measure nonlinear effects
 - identify differences between the two types of packaging tested
 - present data in a form suitable for use in validation of computer program FRATE
- (2) Response Testing
 - quantify responses of carbody and lading for given track conditions

Data processing was accomplished at three levels:

- (1) Data available during and immediately following each run:
 - sight and sound observations including video displays
 - Brush recordings of selected measurements (primarily lading accelerometers)
 - oscillograph records of selected measurements
 - Hewlett-Packard analyzer spectrum and transfer function plots of one or two measurements
- (2) Data available within one or two days after each run
 - Bode plots of selected measurements (These were frequency spectra of the ratio of response/input acceleration measurement showing both amplitude ratio and phase angle.)
 - PSD (Power Spectral Density) of selected measurements-used for random vibration tests
- (3) Final Data:
 - Bode plots of all requested measurements
 - Modal analysis results-- this consists of Argand (circle curve fitting) plots & modal amplitudes (print and plot)

The RDL has several packaged computer programs that are used in the analysis of data. The Bode plot package will plot response amplitude and phase angle against frequency. The response can be as measured values or expressed as ratios using a reference measurement. The phase angle of the response relative to the reference measurement is plotted on the same sheet of paper with the response data, with the frequency axes aligned for easy reference between amplitude and phase angle. Bode plots can be generated from sine sweep test or from random test data. In-phase and quadrature phase (CO/QUAD) vs frequency, Power Spectral Density, Coherence Function and Time Histories are also available.

The Structural Dynamics Research Corp. (SDRC) Modal Plus Package was used for the most part in obtaining modal data. This consisted of CO/QUAD plots with least square, circle fitting (Argand plots) to determine modal frequency, amplitudes and damping with tabular and graphic outputs. The data analysis capabilities are discussed briefly in Reference 3.

The test requirements and test procedures defined in References 6 and 7 contain specific details both as to tests to be performed and data to be measured, recorded and processed. The data details included definition for each run as to what measurements would be processed for each phase (immediate, quick look, and final) and which processed data forms were to be accomplished.

The general data handling procedure was to first verify that the objectives of each run were accomplished. In the case of the modal test this would mean that sufficient data was available and reviewed to determine that target resonance had been found and data required for final analysis had been properly recorded. In the case of response testing, the immediate data would be reviewed to verify that the input was as required, that there were no anomalies needing explanation before proceeding and that data were recorded for final analysis. At the completion of each run, the immediately available data was reviewed and the decision made to continue, repeat the run, or repeat the run with changes.

The quick look data were reviewed as they became available to verify or correct conclusions based on immediate data and to verify that there were no problems with the data recordings.

6. RESULTS OF DATA ANALYSIS

Tests were performed for each loaded configuration to obtain information on 12 separate characteristics:

- first carbody roll
- second carbody roll
- carbody yaw
- carbody bounce
- carbody pitch
- carbody torsion
- carbody bending
- lading lateral resonance
- lading vertical resonance
- response to staggered rail
- response to hunting motion
- response to hump-in-rail

Test results on each of these characteristics are presented and discussed in this section.

6.1 First Roll Mode

The action of the suspension system with the carbody in roll motion is very nonlinear. There are four motions which may be involved:

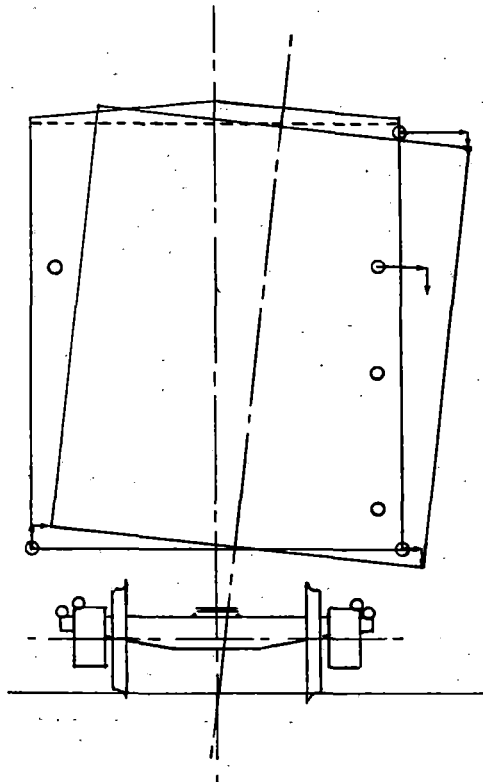
- seated centerplate
- rocking centerplate

- side bearing contact
- centerplate lifted

Furthermore, each of these four motions will be complicated by the following conditions:

- friction snubbers locked or sliding
- lateral motion of the truck bolster between gib stops
- rocking motions of the side frames

Spring rates and snubber forces under most of these conditions were determined in the testing of Reference 1 and are presented in detail in that report. The modal vibration testing of this report does not provide a separation of the effects of these various conditions but does show the net results as to resonant frequency and overall motion of the carbody. In every case tested, it was found that the carbody motion in the first roll mode was one of rocking with the center of rotation about an axis half way between the rails and at a height adjacent to the top of the rail. Figure 6.1 illustrates the roll deflection.



Run 30 Configuration 1B Modal Analysis
 $f = .677 \text{ Hz}$ $\zeta = .0302$ (Damping Factor)

FIGURE 6.1 CARBODY ROLL MOTION IN FIRST ROLL MODE

The frequency of the roll mode varied as a function of gross weight, amplitude of motion, snubber condition and type of test (up sweep, down sweep or decay). Table 6-1 is a summary of frequencies identified for each of the conditions tested. This data was used to generate the curves shown in Figure 6.2 which will now be discussed in detail.

The input motion in these tests consisted of vertical sinusoidal displacements at the rail with each side moving together and out of phase with the other side. Thus, a sinusoidal vertical motion of + 0.10 inches of each rail results in cross level variations of + 0.20 inches and a maximum cross level difference of 0.40 inches.

The loaded boxcar without snubbers, Configuration 1B, is seen in Figure 6.2 to have the first roll mode to range between 0.69 Hertz for small input motions, to an extrapolated 0.60 Hertz for 0.75 inch cross level difference. The decreasing frequency with increasing amplitude, is the expected softening nonlinear spring characteristic of a rocking centerplate. The difference of about 0.05 Hertz (8%) between up sweep and down sweep is again the expected effect of the nonlinear spring characteristic.

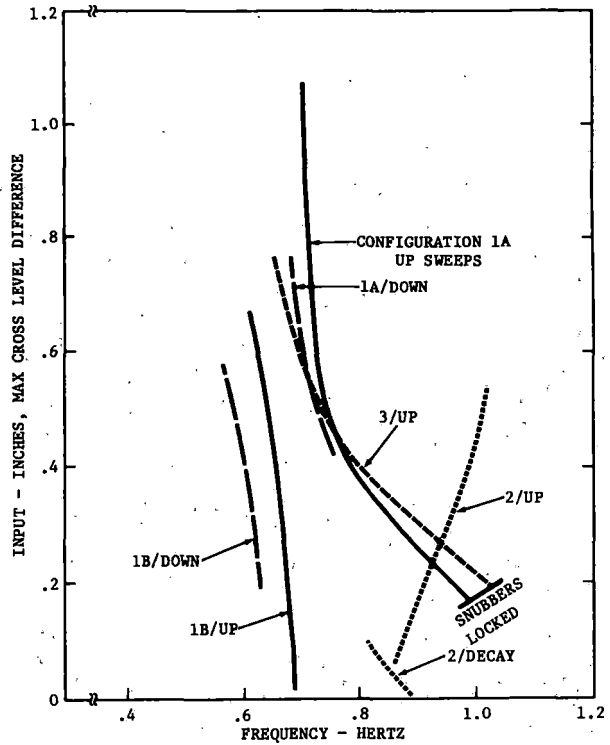


FIGURE 6.2 SUMMARY PLOT OF FIRST ROLL MODE FREQUENCIES

TABLE 6-1 FREQUENCY SUMMARY - FIRST ROLL MODE

Config.	Test	Input	Frequency Hertz	Damping (C/Cc)	Notes	Run No.
1A	Up Sweep	+ .05 in	.96	--	O Graph/Vis.	8
1A	Down Sweep	+ .15 in	.7013	.0468		9B
1A	Up Sweep	+ .15 in	.7215	.0069		59A
1A	Down Sweep	+ .15 in	.6887	.1005	Argon Plots	59B
1A	Up Sweep	+ .25 in	.70	--	O Graph/Vis.	10
1B	Decay	--	.67-.70	.02		46
1B	Up Sweep	+ .05 in	.677	.0302		30
1B	Up Sweep	+ .10 in	.658	.0318		32
1B	Down Sweep	+ .10 in	.579	.0323		32
1B	Up Sweep	+ .15 in	--	--	Aborted--Too Large	31
2	Decay	--	.81-.89	.042-.048	O Graph/Vis	64
2	Sweep	+ .05 in	.906	.045	Modal Anal	72
2	Sweep	+ .10 in	.98-1.00	--	O Graph/Vis	71
3	Up Sweep	+ .05 in	1.02	--	Snub Squeaks Twice	100
3	Up Sweep	+ .15 in	.688	.0659	Snub Break @ .71 Hertz	101

The effect of adding friction snubbers, comparing 1B (without snubbers) to 1A (with snubbers), is seen to raise the resonant frequency. At an input of 0.60 inches cross level difference, the with-snubber frequency is about 0.10 Hertz (or 14%) higher than that without. At lower levels of input the snubbers are seen to have an increasing effect in raising the roll frequency. At 0.20 inches input the difference is about 0.28 Hertz, or 29%. For levels of input below 0.20 inches cross level difference the snubbers remain locked and the roll frequency jumps upward to an undetermined value.

The difference between up sweep and down sweep is less with snubbers than without. The difference in roll response due to the change in packaging, comparing 1A to 3, is within the range of data scatter and is not significant.

In Configuration 2 (empty, no snubber), the response motions were at larger amplitudes, to the point that both side bearing and gib clearances were exceeded. As a result, the resonant frequency curve shows a softening nonlinear (decreasing frequency) spring characteristic for input amplitudes below 0.10 inches and a hardening nonlinear (increasing frequency) for input motions greater than 0.10 inches (see Figure 6.2).

To reiterate this section's opening statement, the freight car suspension system is very nonlinear when in roll motions. The most significant contributors to nonlinearity are the friction snubbers, the transition from seated to rocking centerplate and the effects of side bearing contact. The effects of each of these contributions vary with amplitude of motion.

The computer program FRATE presently uses an average value for the seated-rocking centerplate condition. This is considered an accurate simulation for conditions other than small amplitudes of roll motion. Since small amplitude motions do not present a problem that needs to be addressed, this assumption in FRATE does not detract from its utility. FRATE does simulate the side bearing contact transition and does model the friction snubber with coulomb damping. Consequently, validation for roll motions will essentially require the adjustment of coefficients in the model.

6.2 Second Roll Mode

The second roll mode motion consists of rigid body roll of the carbody about a center of rotation that is somewhere near the center of gravity of the carbody and contents. The mode is strongly influenced and subdued by the snubbers to the extent that in Configuration 1A it had not been found by the time the planned testing had been completed. It was concluded that in order to find the mode it would be necessary to go to higher frequencies as well as larger input amplitudes. However, it was decided to discontinue this search and rely on the results of Configurations 1B and 3 (stretch wrap packaging and with friction snubbers) for definition of this mode. The second roll mode in Configuration 3 should be essentially the same as Configuration 1A. Table 6-2 contains a summary of test results for the second roll mode.

In Configuration 1B, the second roll mode was obtained for two levels of input and was found to increase in frequency with increase in input level. This variation is shown in Figure 6.3. The deflection shape, shown in Figure 6.4, is a rigid body rolling motion of the carbody about an axis that is about 106 inches above the top of rail and about 22 inches above the center of gravity of the carbody and contents.

The change from Configuration 1B to 2 was from the loaded to the empty condition. The weight was reduced to about 39% and, based on data in Reference 1, the suspension stiffness was reduced to about 56% of the loaded values. The frequency change can be estimated by the square root of the ratio of stiffness over weight changes; thus, the Configuration 1B frequency of 2.6 Hertz would be expected to change to 3.1 Hertz for Configuration 2.

The second roll mode for Configuration 2 was obtained by performing decay tests. The frequency was determined to be 3.04 Hertz compared to the expected 3.1. The mode shape obtained is shown in Figure 6.5 and is seen to be a roll motion of the carbody about an axis that is about 100 inches from top of rail (the center of gravity of the carbody is about 67 inches above top of rail).

In Configuration 3, the frequency jumped to 3.89 Hertz and the center of rotation shifted down to the plane of the center plate as can be seen in Figure 6.6.

TABLE 6-2 FREQUENCY SUMMARY--SECOND ROLL MODE

Config.	Test	Input	Frequency (Hertz)	Damping (C/Cc)	Notes	Run
1A	Up Sweep	$\pm .1$ in	Max Freq = 3.0 Hz Max Amp not Reached		$f = 3$ Hz	11
1A	Up Sweep	$\pm .3$ in	No Records			12
1A	Up/Dn Sweep	$\pm .2$ in	Max Amp not Reached		$f = 3$ Hz	14
1B	Up Sweep	$\pm .2$ in	3.00 (Up) 2.94 (Dn)		0 Graph/Vis	33
1B	Up/Dn Sweep	$\pm .05$ in	2.630 (Up) 2.525 (Dn) 2.60 (Up) 2.54 (Dn)	.0304 .0266	Modal Anal 0 Graph/Vis	34/35
2	Decay	$\pm .10$ in	2.7	.03	Decay	65
2	Decay	$\pm .05$ in	3.0	.06	Decay	66
3	Up Sweep	$\pm .2$ in	3.0 or		0 Graph/Vis	102
3	Up Sweep	$\pm .1$ in	3.0-3.5 3.89	.0429	0 Graph/Vis Modal	103

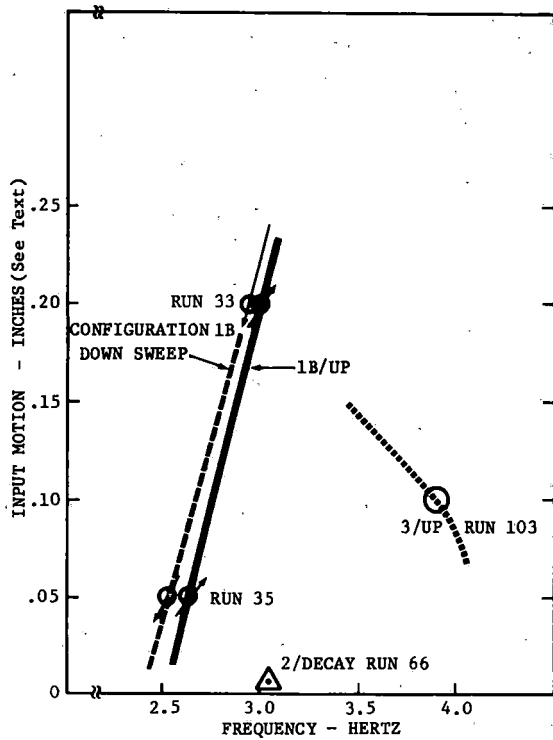


FIGURE 6.3 SUMMARY PLOT OF SECOND ROLL MODE FREQUENCIES

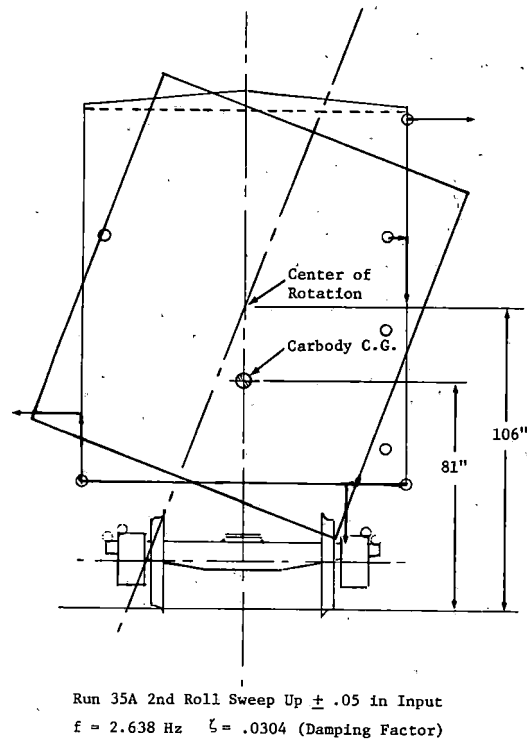


FIGURE 6.4 CARBODY ROLL MOTION IN SECOND ROLL MODE, CONFIGURATION 1B

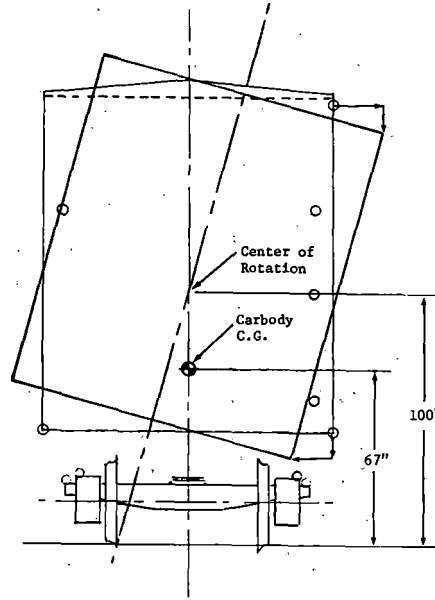
In the change from Configuration 1B to 3 the total lading was decreased by 1140 pounds and the lading height dropped about 8 inches. The combined effect of those two changes was to lower the roll inertia of carbody and contents by about 5% and in turn cause the second roll frequency to be higher by about 2.5%, a change from 2.6 to about 2.7 Hertz. It was, therefore, assumed that the actual change from 2.6 to 3.89 Hertz as well as the shift in the center of rotation was primarily due to the influence of the friction snubbers.

The action of the friction snubbers is to lock each end of the truck bolster to its respective side frame until dynamic forces exceed the snubber friction force. The snubbers will slide only as long as the dynamic force is greater than the friction force. Under these changing conditions the suspension stiffnesses (lateral, vertical and roll) are either very high, because one or both spring nests are locked out by the snubber or are equal to the spring nest spring rates.

For small dynamic motions the friction snubbers remain locked and the effective suspension system is very stiff. As the dynamic motions are increased a level will be reached where the friction forces are exceeded and the snubbers start to move. Thus, in each cycle of the dynamic motion there is a portion where the suspension is stiff and a portion where the suspension is soft and the combined effective stiffness is a weighted average of the two conditions. As the amplitude of motion is increased the portion of each cycle with sliding snubber will increase and the effective stiffness is decreased.

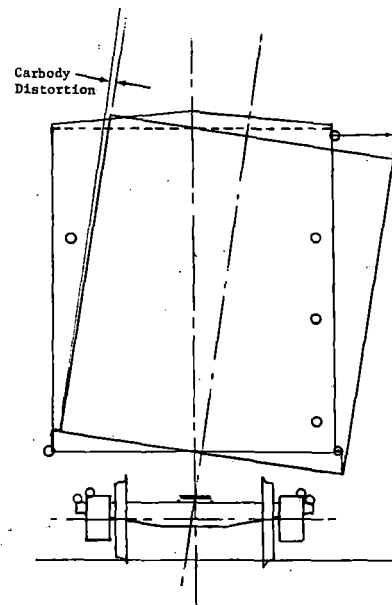
It must therefore be concluded that the second roll mode will change with amplitude of motion both as to resonant frequency and center of rotation: for increased amplitudes the frequency will decrease and the center of rotation will go up. The results obtained for Configuration 1B and 3 are concluded to be the limits of this variation: 1B test results without snubbers are assumed to be the limit condition for very large amplitudes of motion with snubbers; Configuration 3 test results represent the other extreme of relatively small amplitudes of motion and where the snubbers are sliding a small portion of each cycle.

There was some carbody distortion noted in the deflection shape for Configuration 3, Figure 6.6, which was not found in any of the other roll modes. Its presence was probably due to the high frequency (3.89 Hertz) and the low center of rotation. This amount of distortion is to be expected and its presence is pointed out as a passing observation.



Configuration 2 Second Roll From Decay of Run 66
 $f = 3.04$ Hz

FIGURE 6.5 CARBODY ROLL MOTION IN SECOND ROLL MODE, CONFIGURATION 2



Run 103 Sweep Up ± 0.10 in. Input Modal Analysis:
 $f = 3.89$ Hz $\zeta = .043$ (Modal Damping Factor)

FIGURE 6.6 CARBODY ROLL MOTION IN SECOND ROLL MODE, CONFIGURATION 3

6.3 Yaw Mode

The yaw mode was similar to the second roll mode in that the snubbers had an overpowering effect. In both Configurations 1A and 3 the snubbers remained locked throughout the testing, which in both cases was from 0.5 to 6.0 Hertz. There was no detectable yaw mode in Configuration 1A. In Configuration 3 the yaw mode was determined to be at 6.0 Hertz.

In the two configurations without snubbers, 1B and 2, the yaw mode frequency was found to fall in the 1.6 to 2.6 Hertz range. Figure 6.7 shows variations of frequency with amplitude of input. The relative amplitudes of lateral motion of carbody, lading and trucks are shown in Figure 6.8 while yaw motion of the carbody is shown in Figure 6.9.

The lading lateral resonance, with the yaw mode locked out by the snubbers, was found to be between 1.6 and 2.6 Hertz depending on the amplitudes of motion (see Section 6.8). The net effect, as found in Configuration 1B testing, is a highly coupled carbody yaw/lading lateral mode between 1.65 and 1.71 Hertz.

It must be concluded for the general case that the carbody yaw resonance can be anywhere from 1.5 to 6.0 Hertz depending on amplitude of the yaw motion generated (body hunting), the condition of the friction snubbers, the vehicle gross weight, and dynamic properties of the lading. It is also likely that the yaw mode behavior is similar to the bounce mode in that there is some critical amplitude of yaw motion beyond which the motions increase abruptly to violent levels. This is discussed further in the following section (bounce mode).

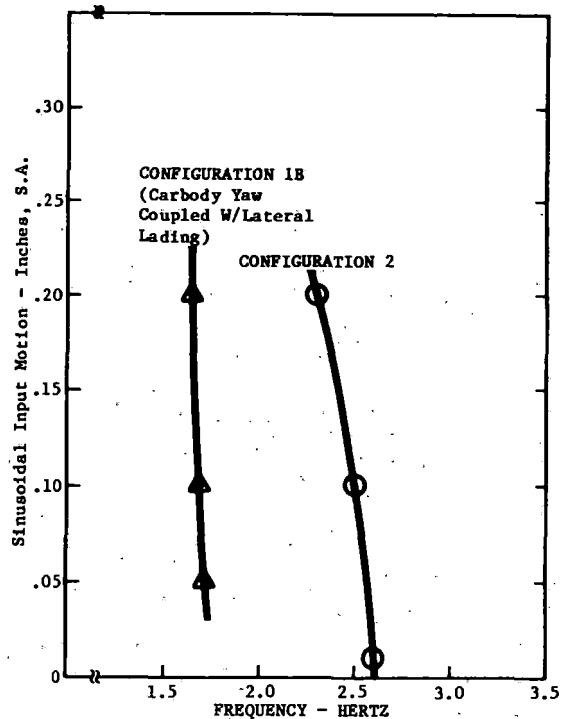
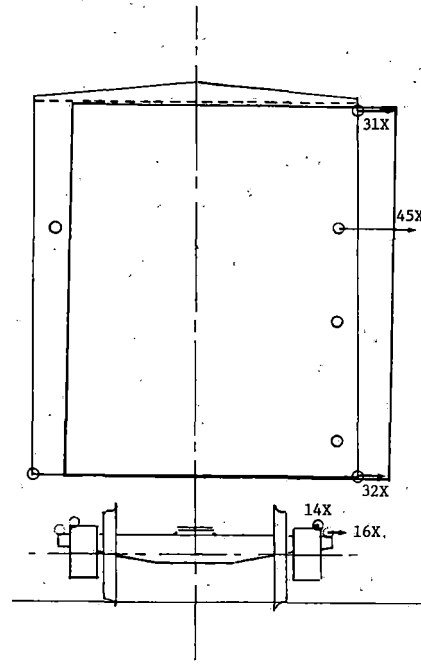


FIGURE 6.7 CARBODY YAW MODE FREQUENCY SUMMARY



B End of Vehicle Lateral Motion (Relative Amplitudes)			
45X Top of Lading	14.12	31X Top of Carbody	6.73
32X Bottom of Carbody	5.81	16X Bolster	4.41
14X Sideframe	- .49		

FIGURE 6.8 RELATIVE LATERAL MOTIONS IN YAW MODE, CONFIGURATION 1B, $f = 1.708 \text{ Hz}$

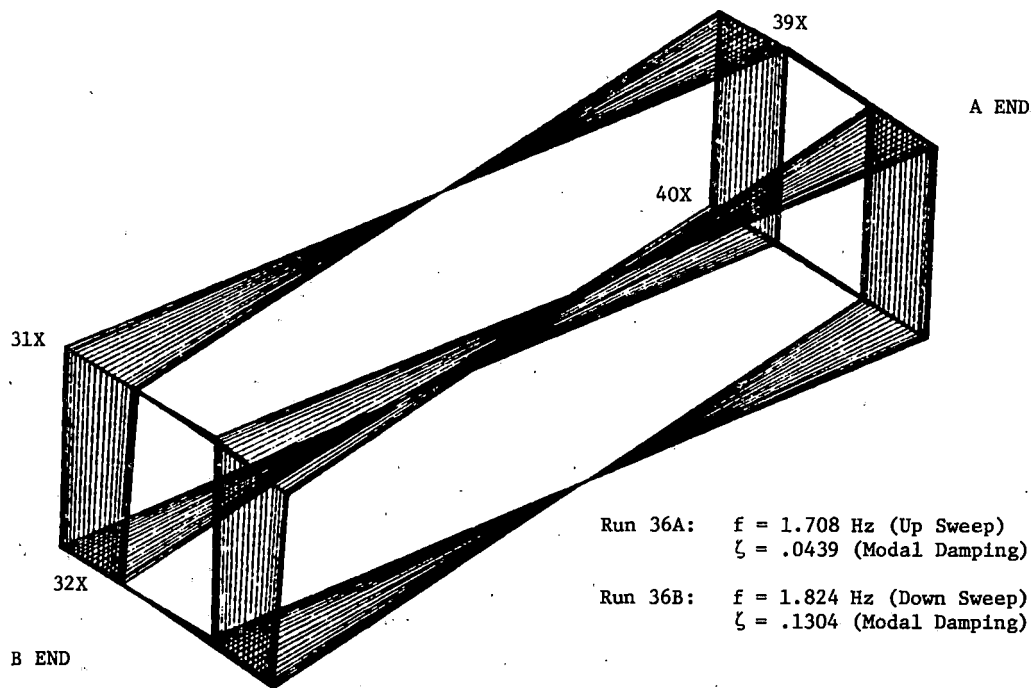


FIGURE 6.9 YAW MODE SHAPE, CONFIGURATION 1B

TABLE 6-3 FREQUENCY SUMMARY--BOUNCE MODE

Config	TEST	Input (+ in.)	Bounce Mode		Notes	Run
			Freq. (Hz)	Damping (C/Cc)		
1A	Up Sweep $\Delta f = .2$	0.10	(Suppressed By Snubbers)		Q = 1.4 when snubbers start to slide at 3.4 Hertz	15
1A	Up Sweep $\Delta f = .2$	0.20	(Suppressed By Snubbers)		Q = 3.35 when snubbers start to slide at 2.8 Hz Q = 4.2 when carbody motion becomes pitch at 3.0 Hz	16,57
1A	Up Sweep $\Delta f = .1$	0.20	(Suppressed By Snubbers)		Q = 2.35 when snubbers start to slide at 2.6 Hz Q = 2.56 when carbody motion becomes pitch at 3.0 Hz.	21
1B	Decay	0.05	2.05	.005	Q = 7.5 @ 2.0 Hz	39
2	Decay	0.03	3.81	.02	Q = 26.7 @ 3.7 Hz	78
3	Up Sweep	0.20	(Suppressed By Snubbers)		Q = 3.74 @ 2.8 Hz when snubbers start to slide & carbody motion changes from bounce to pitch	104
3	Up Sweep	0.30	(Below 2.39 Hz)		Snubbers start to slide @ 2.39 Hz. Carbody response 1.5" (Q=5); test stopped to avoid damage	107
3	Up Sweep	0.23	(Below 2.39 Hz)		Snubbers start to slide @ 2.39 Hz. Carbody response @ 1.2 in (Q=5.2)	108

6.4 Bounce Mode

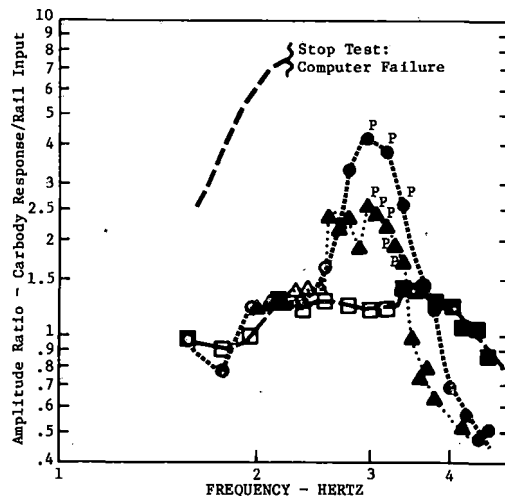
A summary of the results of bounce mode testing is given in Table 6-3 and the frequency response curves are shown in Figures 6.10 and 6.11.

Without snubbers the bounce mode was easily found by the decay test method. The mode was at 2.05 Hertz in Configuration 1B and 3.81 in Configuration 2.

The bounce mode was suppressed by the snubbers to a degree that is dependent on the amplitude of the input motion. In Configuration 1A with 0.10 inches input at the rails (see Figure 6.10), the response is essentially flat through the frequency range tested, with a small step up at 3.4 Hertz where the snubbers start to slide. At the input level of 0.20 inches the snubbers start to slide in the 2.6 to 2.8 Hertz range and, because of being closer to the bounce mode frequency, the response amplitude ratio is larger. The response is further complicated in that the carbody pitch mode is near 3.0 Hertz and the carbody motion changes from bounce to pitch when the excitation frequency is near that frequency.

There were three levels of input tested in Configuration 3: 0.20, 0.30 and 0.23 inches. The data are summarized in Figure 6.11. The 0.20 level was tested first and the results were very similar to Configuration 1A; in both cases the response was low through what was the bounce mode without snubbers and then jumped to a carbody response/rail input ratio of between 3.5 and 4.0 after which the carbody motion changed from bounce to pitch. At the 0.30 input level the snubbers started to slide at 2.4 Hertz and quickly reached amplitudes that were large enough that the test director stopped the test to avoid damage. At the 0.23 inch input level the snubbers again started to move at 2.4 Hertz and the response again jumped to a high level. But in this case the response fell off at frequencies above 2.4 Hertz and the carbody motion did not change from bounce to pitch. Figure 6.12 shows the variation of the bounce mode frequency with input level changes for Configuration 3. The figure also notes the decay test results for Configuration 1B and 2.

In summary the snubbers very effectively suppress the bounce mode for low level of input at the rails. However, above some critical input level the responses will quickly become dangerously large. For a sinusoidal input near the bounce mode of 2.05 Hertz this critical level is about ± 0.25 inches.

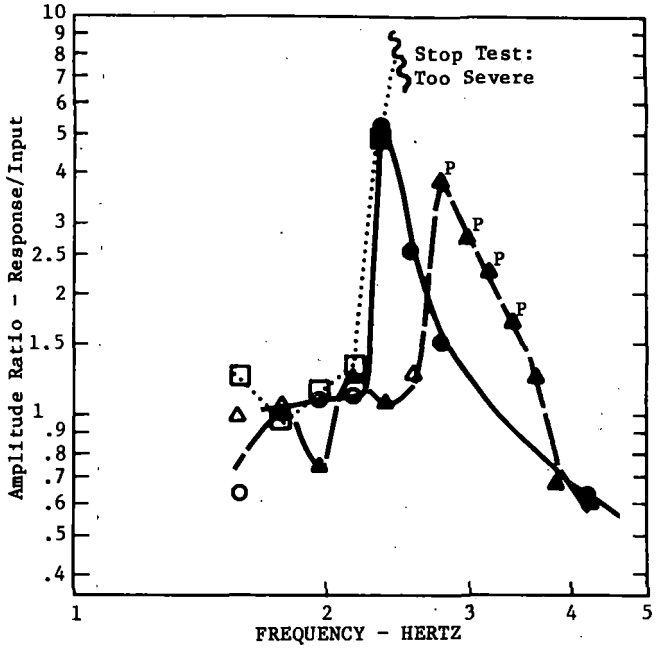


Test Condition Legend

Run	Config.	Input (+ in.)	Δf (Hertz)	Snubber	
				Locked	Sliding
15	1A	0.10	0.20		
17	1A	0.20	0.20		
21	1A	0.20	0.10		
38	1B	0.20	0.20	No Snubber	

P = Motion has changed from Bounce to Pitch

FIGURE 6.10 BOUNCE TEST RESPONSES, CONFIGURATIONS 1A & 1B



Test Condition Legend - Configuration 3

Run No.	Input (+ in.)	Snubbers	
		Locked	Sliding
104	0.20	—▲—	—▲—
108	0.23	—○—	—●—
107	0.30□.....■.....

P = Motion has changed from Bounce to Pitch

FIGURE 6.11 BOUNCE TEST RESPONSES, CONFIGURATION 3

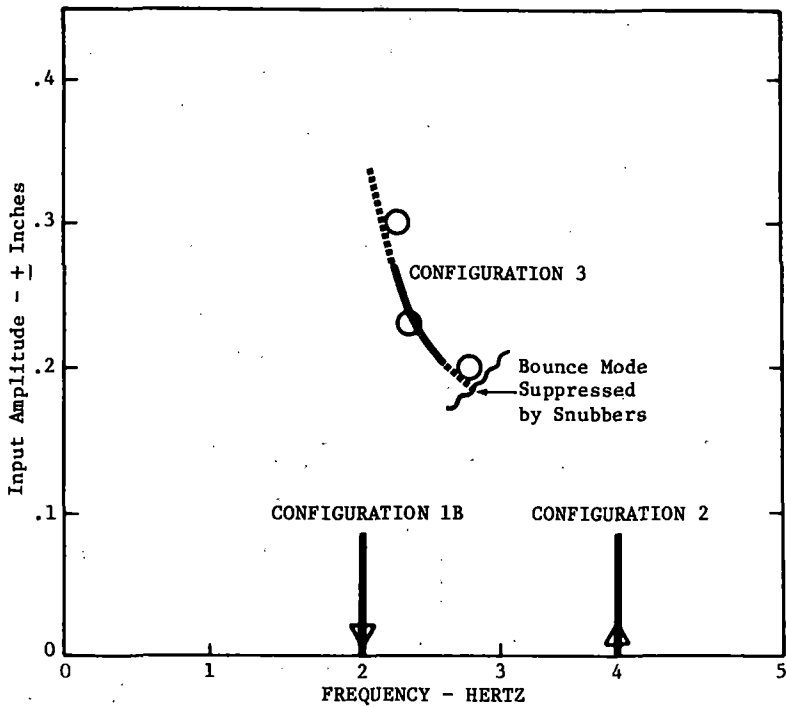


FIGURE 6.12 BOUNCE MODE FREQUENCY VARIATIONS

6.5 Pitch Mode

The pitch mode behavior was much like the bounce mode in that without snubbers the mode was easily found with decay tests and with snubbers the mode was suppressed to a degree that varied with the level of input motion. Table 6-4 contains a summary of the frequencies identified. The data are also plotted in Figure 6.13 showing graphically how the snubbers and input levels work

together to cause variation of the pitch mode frequency.

The input levels were not increased to higher levels as they were in the bounce mode testing, however it is very likely that the behavior is the same. That is, as the level of input motion is increased beyond + 0.25 inches the pitch motion of the carbody will quickly increase to destructive amplitudes.

TABLE 6-4 FREQUENCY SUMMARY--PITCH MODE

Config.	Test	Input (+ .in)	Pitch Mode		Notes	Run No.
			(Freq/Hz)	(C/Cc)		
1A	Up Sweep	0.1	3.0		Snubber breaks @ 4.46 Hz (90° @ 5.5 Hz)	19
1A	Up Sweep	0.2	3.805	.049	RDL Modal Anal./Snubber breaks @ 3.63 Hz (90° @ 4.3 Hz)	20
1B	Decay	0.1	2.77	.047	From O'Graph data	42
2	Decay	0.15	4.34	.015	From O'Graph data	80
3	Up Sweep	0.2	3.696	.014	RDL Modal Anal.	106

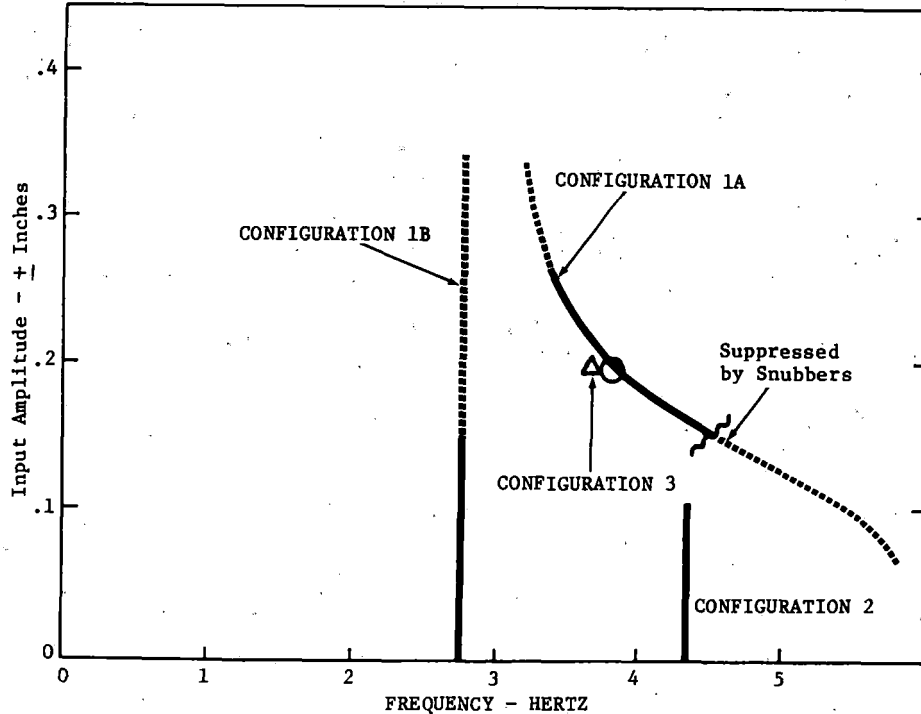


FIGURE 6.13 PITCH FREQUENCY VARIATIONS

6.6 Body Torsion Mode

Two carbody torsion modes were found for each configuration tested and have been designated here as Torsion Mode 1 and Torsion Mode 2. Mode 1 occurs at a slightly lower frequency than Mode 2 and is coupled with a yawing motion of the carbody. Mode 2 is more representative of an uncoupled torsion mode. A summary of the frequencies identified is given in Table 6-5 and deflection shapes representative of each mode are shown in Figures 6.14 and 6.15.

The objective of testing the cars with doors open, (Run 3) and doors closed, (Run 4), was to show that the doors had little effect on body stiffness. This would allow all runs to be made with doors open thus permitting observations of the behavior of the lading during the tests. This hypothesis was proven when the torsion frequencies changed less than three percent in Mode 1 and four percent in Mode 2. However, the direction of the frequency change indicated that the carbody was stiffer when the doors were open. This is opposite from the expected and no logical explanation has been found.

A second finding that was not expected was that the carbody torsion modes were essentially the same for empty and loaded conditions. The lading has its own resonant frequencies, about 2 Hertz lateral and 8 Hertz vertical, and a major portion of the lading mass is isolated at the torsion mode frequencies. That is, the pallets are acting as soft springs in the 12-15 Hertz range permitting the lading to be stationary relative to the motion of the floor. However, there is some portion of the lading which does move with the carbody floor and its mass would be expected to lower the torsion frequencies. Furthermore, the motion of the lading measured is large enough, even though smaller than the carbody motion, to expect that the lading would influence the torsion mode.

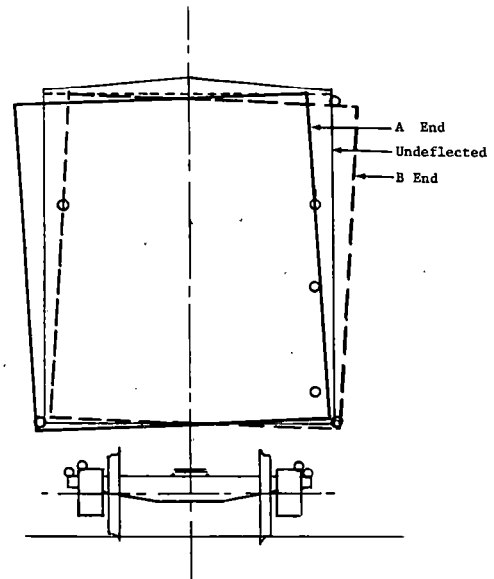


FIGURE 6.14 BODY TORSION MODE DEFLECTION SHAPE CONFIGURATION 1A, 12.72 Hz

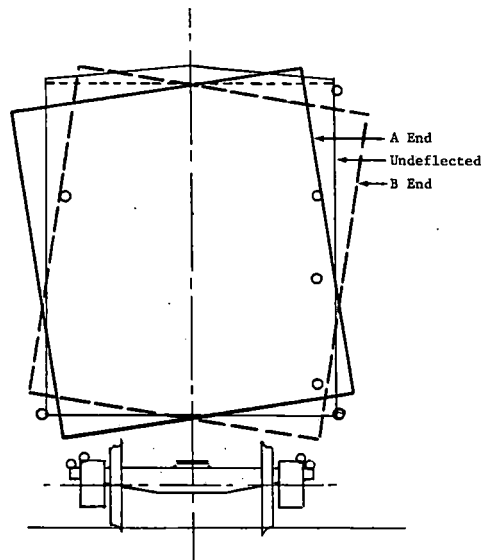


FIGURE 6.15 BODY TORSION MODE DEFLECTION SHAPE CONFIGURATION 1B, 15.36 Hz

TABLE 6-5 BODY TORSION MODE FREQUENCIES

Config.	Mode 1(1) Hertz/C/Cc	Mode 2 Hertz/C/Cc	Run No.
1A (Car Door Open)	12.72/.1012	14.7/(2)	3
1A (Car Door Closed)	12.44/.1065	14.1/(2)	4
1B	13.67/(2)	15.36/.0805	37
2	13.125/.0146	14.75/(2)	81
3	13.17/.1022	14.8/(2)	99

- (1) Mode 1 and Mode 2 as designated here are both apparent body torsion modes. Mode 1 is coupled with carbody yaw (see Figure 6.14) where Mode 2 has the appearance of uncoupled body torsion (Figure 6.15).
- (2) These frequencies were obtained from frequency response plots or oscillographs and no damping values were obtained.

6.7 Body Bending Mode

There were a number of resonances found in the 12-20 Hertz range in the search for the carbody bending mode. However, in the final evaluation, it was concluded that the bending mode was not found, and was, in fact, above 20.0 Hertz and out of the range of interest.

Modal analyses were performed by the RDL using their modal analysis computer program for modes identified in Runs 18 and 105, Configurations 1A and 3 respectively. These modes were determined to be at 16.86 and 16.79 Hertz. The deflection shapes are shown in Figure 6.16. These deflection shapes are representative of a bounce mode with some body bending and not of a true bending mode. Further explanation is found by referring back to the bounce mode data in Section 6.4. The bounce mode was found to be between 2.0 and 2.5 Hertz depending on the amplitude of input, and providing the input level was above the threshold level to cause the friction snubbers to slide. At lower input levels, that is, with the friction snubbers locked, the vertical suspension system increases in stiffness by a factor of about 50 (from Reference 1). This stiffness increase would cause the bounce mode to shift from 2.0-2.5 Hertz to 14-18 Hertz. With these two corroborating pieces of data, i.e. the expected frequency of carbody bounce with locked snubbers match the modes of Figure 6.16 and the deflection shapes measured are representative of bounce modes, it was concluded that the Figure 6.16 modes initially identified as carbody bending are actually locked snubber bounce modes and further that the carbody bending mode is at some higher frequency.

Some of the other resonances noted in the 12-20 Hertz range were identified from visual observations to be local resonances of carbody side panels, the roof and the doors. Since measurement of these resonances was not an objective of this test the instrumentation was not of the number and location needed to characterize them.

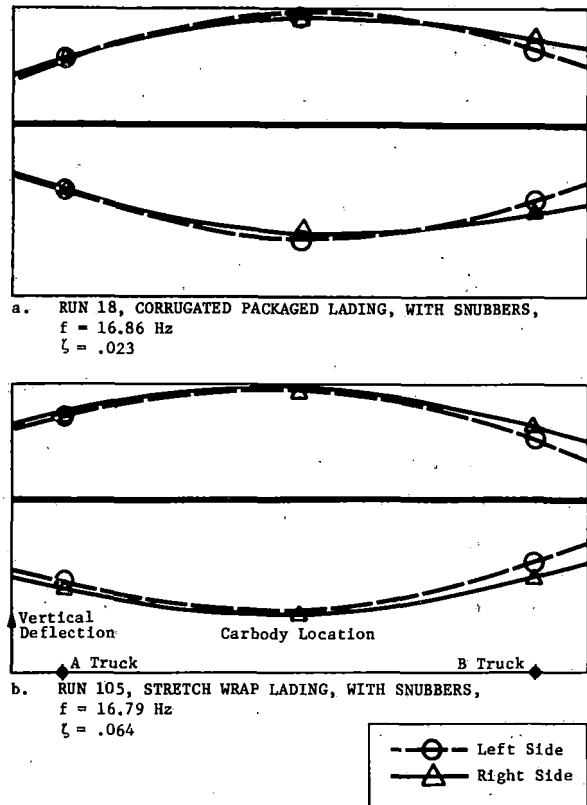


FIGURE 6.16 CARBODY BENDING MODE DEFLECTION SHAPES

6.8. Lading Modes

General Observations

The apparent physical differences between corrugated paper and stretch wrap packaging is that the stretch wrap is stiffer and tighter. Stretch wrap is stiffer in that deflections under load in any direction are less, and tighter in that the cans in the packages have less relative motion between each other. One would expect that the resonant characteristics in pallet stacks would be quite different --stretch wrap at a higher frequency and with less damping. Vibration test results do not show a significant difference within the data scatter. (Data scatter caused by differences between location in the car and by differences in the car configuration.) The explanation of this unexpected

behavior is that the stacked lading resonant characteristics are apparently determined by the pallet and not the lading packaging. With the same pallet and the same weight lading, the resonances are essentially the same.

6.8.1 Lateral Lading Mode

The lateral resonance mode of the lading was found by performing frequency sweeps with sinusoidal yaw motions input at the wheels. That is, lateral sinusoidal motion was applied at each axle with a 180° phase difference between the A and B trucks. The hunting simulation used the same input motions and those results were used to identify the lading resonance as well as the resonance search runs. Resonances were identified as being at the frequency of maximum response as shown by oscillograph data

TABLE 6-6 LADING LATERAL MODE RESPONSE DATA

Config.	Input (1) (Inches)	Freq. (2) (Hertz)	Response A45X (3)		Run No.
			Fundamental (g's/in)	Total (g's)	
1A	.05	2.62	.25/0.36	0.29	5
1A	.15	2.16	.45/0.94	0.54	6
1A	.30	1.92	.53/1.41	0.90	7
1A	.2	2.02	.43/1.03	0.53	22
1A	.4	2.00	.55/1.34	1.30	23
1A	.6	1.70	.68/2.30	2.30	24
1B	.05	1.71	.19/0.64	.28	36
1B	.2	1.65	.49/1.76	1.07	49
1B	.1	1.68	.28/0.97	.65	50
3	.2	1.96	.50/1.27	.70	91
3	.4	1.79	.55/1.76	1.85	92
3	.6	1.60	.61/2.33	2.08	93
3	.05	2.27	.30/0.51	.35	97

- (1) Single amplitude of lateral sine motion at each axle, A & B trucks at 180° phase to each other
- (2) Frequency of maximum amplitude of response in fundamental or modal frequency as determined by analyzer
- (3) Amplitude of fundamental obtained by manual filtering of all other frequencies. Measurement A45X is lateral acceleration at top of lading, left side of vehicle, at B end. See Appendix A for measurement locations.

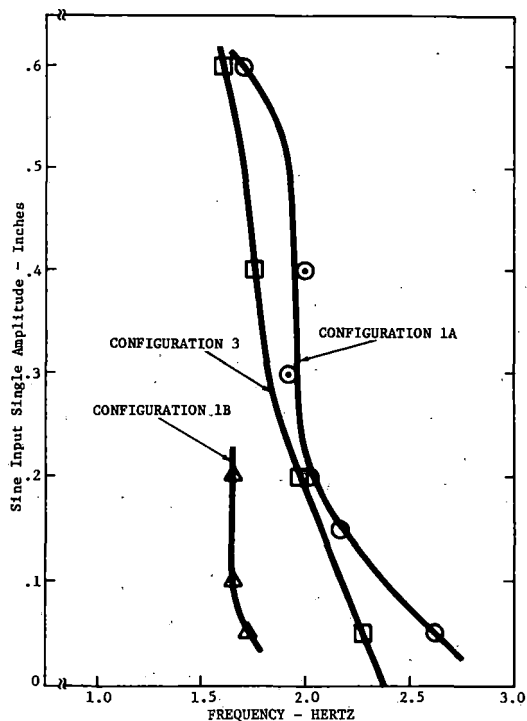


FIGURE 6.17 FREQUENCY SUMMARY, LADING LATERAL MODE, VARIATION WITH INPUT

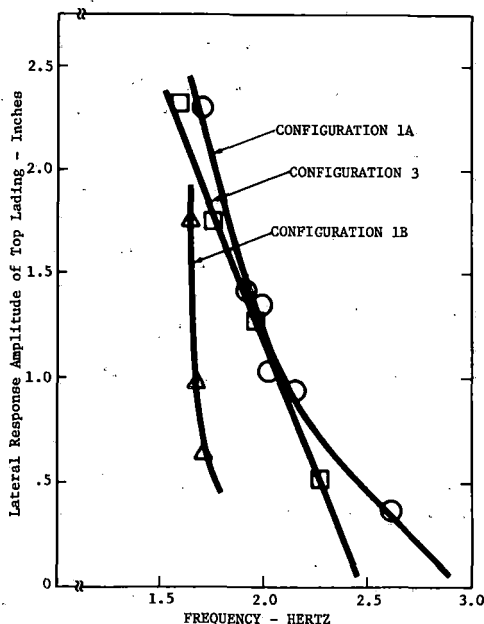


FIGURE 6.18 FREQUENCY SUMMARY, LADING LATERAL MODE, VARIATION WITH RESPONSE

and Bode plots. The computerized modal analysis program was used to identify more accurately the resonant frequency and to define the modal deflection shape.

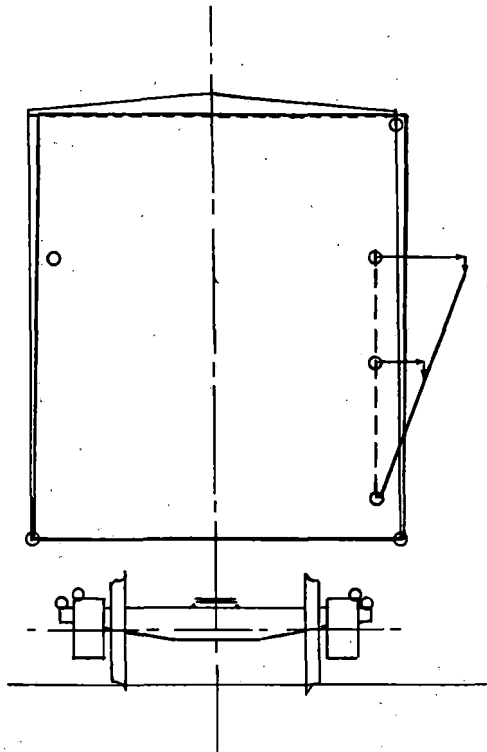
A summary of modal frequencies and responses is given in Table 6-6. The modal frequencies are also plotted in Figure 6.17 against input amplitude and in Figure 6.18 against lading response amplitude. In view of the difference in lading packaging between Configurations 1A (corrugated boxes) and 3 (stretch wrap) there is a surprising degree of similarity of modal frequencies comparing Figure 6.17 and 6.18. The deflection shapes for all three configurations are also very similar, the lading stack rotating as a rigid body about the base, as shown in Figures 6.19, 6.20, 6.21 and 6.22.

These two facts, that the lading mode is not changed in packaging and that the flexibility is concentrated at the base, indicates that the bottom pallet is the controlling flexibility in the lading lateral mode.

The difference between the lading lateral modes for Configurations 1A and 1B is greater than expected since the only change to the test configuration was to remove the friction snubbers. The two results, 1A & 1B, are closer in Figure 6.18 than they are in Figure 6.17 suggesting that frequency variations of these modes are more closely related to response amplitude than input at the rail.

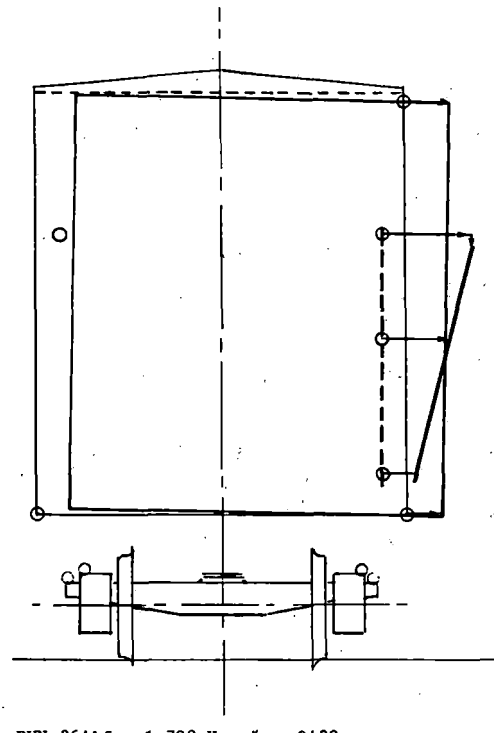
The tendency for the lading lateral mode to decrease in frequency with an increase in amplitude is probably due to the nonlinear nature of the stack, made up of the complex elements of bounce, slide and shearing distortion.

The conclusion was reached that for pallet stack configurations tested the lading lateral mode will vary from 1.5 to 2.5 Hertz and is relatively insensitive to packaging variation.



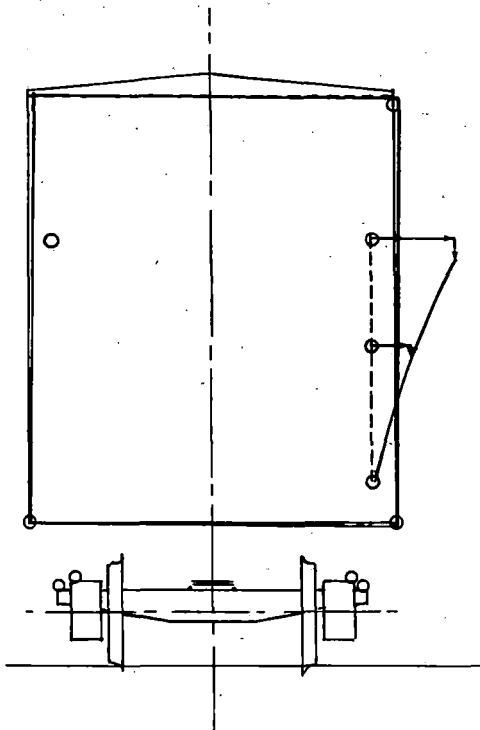
RUN 5: $f = 2.621$ Hz $\zeta = .095$

FIGURE 6.19 LADING LATERAL MODE DEFLECTION SHAPE CONFIGURATION 1A, 0.05 INCH INPUT



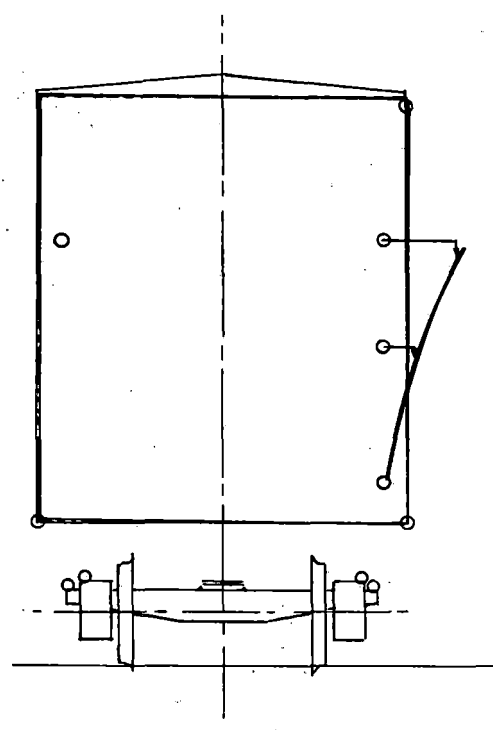
RUN 36A: $f = 1.708$ Hz $\zeta = .0439$

FIGURE 6.21 LADING LATERAL MODE DEFLECTION SHAPE CONFIGURATION 1B, 0.05 INCH INPUT



RUN 6: $f = 2.16$ Hz $\zeta = .063$

FIGURE 6.20 LADING LATERAL MODE DEFLECTION SHAPE CONFIGURATION 1A, 0.15 INCH INPUT



RUN 97: $f = 2.272$ Hz $\zeta = .1431$

FIGURE 6.22 LADING LATERAL MODE DEFLECTION SHAPE CONFIGURATION 3, 0.05 INCH INPUT

6.8.2 Lading Vertical Modes

The vertical resonance mode of the lading was found by performing a frequency sweep, with sinusoidal vertical input at all eight wheels. The input amplitude was controlled to a constant ± 0.30 g's when the input frequency varied from 5.0 to 20.0 Hertz. One run was made for each configuration.

The test data were processed into two forms for analysis: (1) oscillograph records, which present acceleration / time history of selected accelerometers, and (2) response ratio of a larger selection of accelerometers. The response ratio / frequency plots, (Bode plots), were obtained using a wheel accelerometer as the reference. In addition, in order to define better the lading stack characteristics, the vertical accelerometers in the two instrumented stacks at either end of the boxcar were referenced to the vertical accelerometer at the boxcar floor level at the appropriate stack location.

The Bode plots with a wheel accelerometer as reference were determined to have large errors at the lading resonance; that is, the responses indicated were almost two orders of magnitude larger than shown by the oscillograph records and the Bode plots using a boxcar accelerometer as reference. The wheel referenced Bode plots were not used for this reason. The cause of the error was attributed to the high level of harmonic content in the wheel acceleration data.

The lading vertical resonance data is summarized in Table 6-7. The "Q" values given are the ratio of the vertical acceleration at the top of the lading to the vertical acceleration of the carbody floor at the same location. These same data are shown again in the Bode plots in Figures 6.23 through 6.25 for the B End and Figures 6.26 through 6.28 for the A End.

The response curves are seen to be similar in that the resonant frequencies are between 8.5 and 8.7 Hertz, with the peak generally truncated due to package separation. With the separation /truncation, the maximum response frequency varied between 8-9 Hertz as illustrated below.

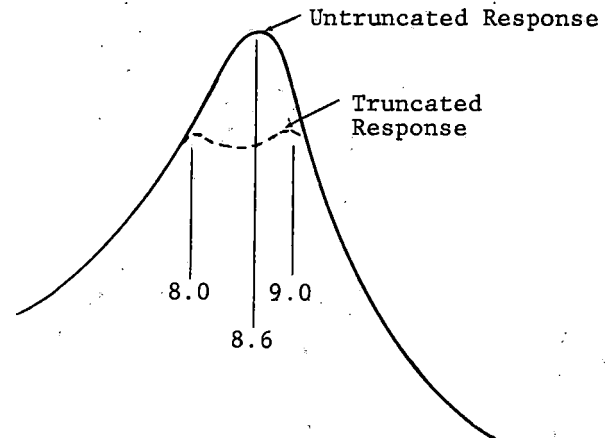


TABLE 6-7 LADING VERTICAL RESONANCE SUMMARY

Config.	B End Lading ⁽¹⁾		A End Lading ⁽¹⁾		Run No.
	Freq. (Hertz)	44Z/33Z (Q)	Freq. (Hertz)	54Z/41Z (Q)	
1A	8.68	11.4	8.50	13.0	18
1B	9.25	10.4	9.00	7.1	40
3	8.25	9.7	8.50	14.4	105

- (1) 44Z - Vertical Accelerometer, Top of Lading, B End
 33Z - Vertical Accelerometer, Carbody Floor, B End
 54Z - Vertical Accelerometer, Top of Lading, A End
 41Z - Vertical Accelerometer, Carbody Floor, A End

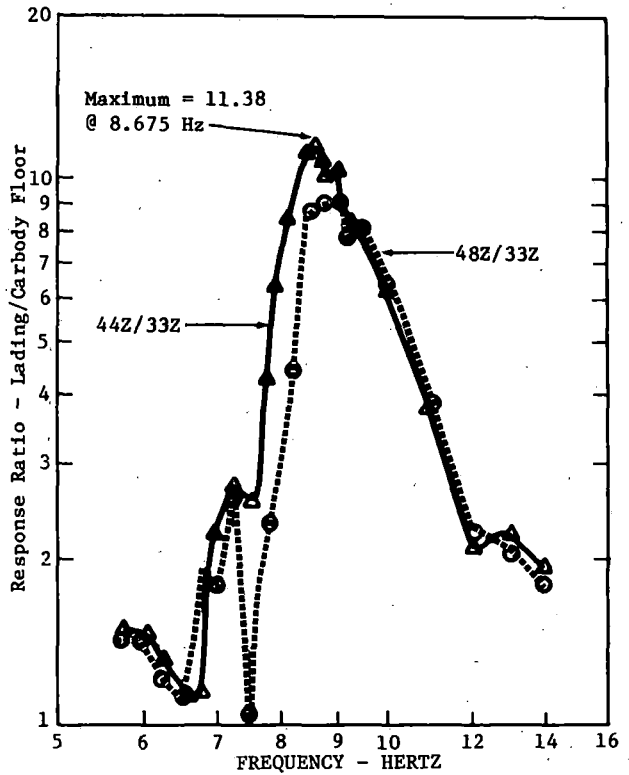


FIGURE 6.23 FREQUENCY RESPONSE, LADING VERTICAL MOTION, CONFIGURATION 1A, B END

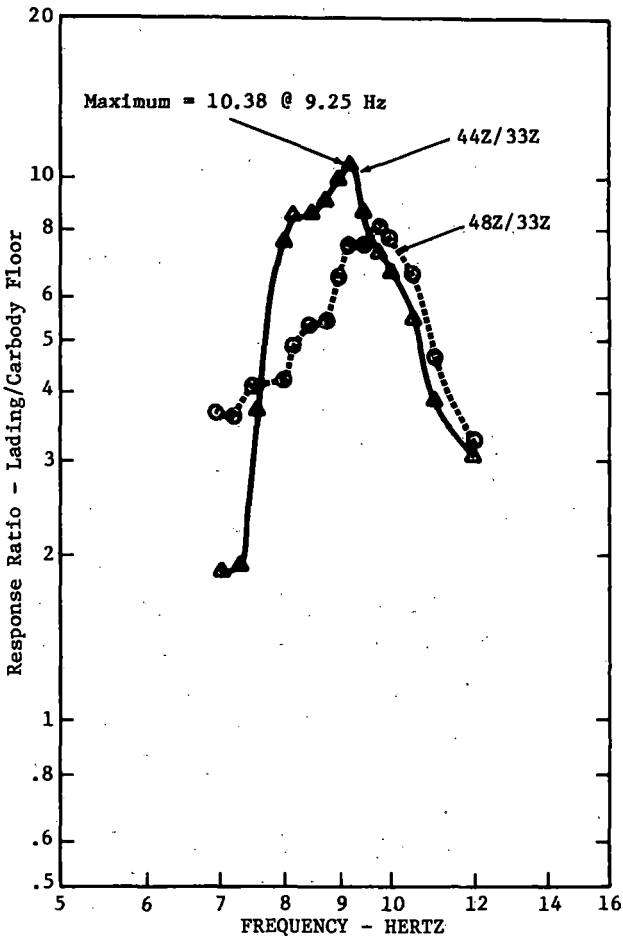


FIGURE 6.24 FREQUENCY RESPONSE, LADING VERTICAL MOTION, CONFIGURATION 1B, B END

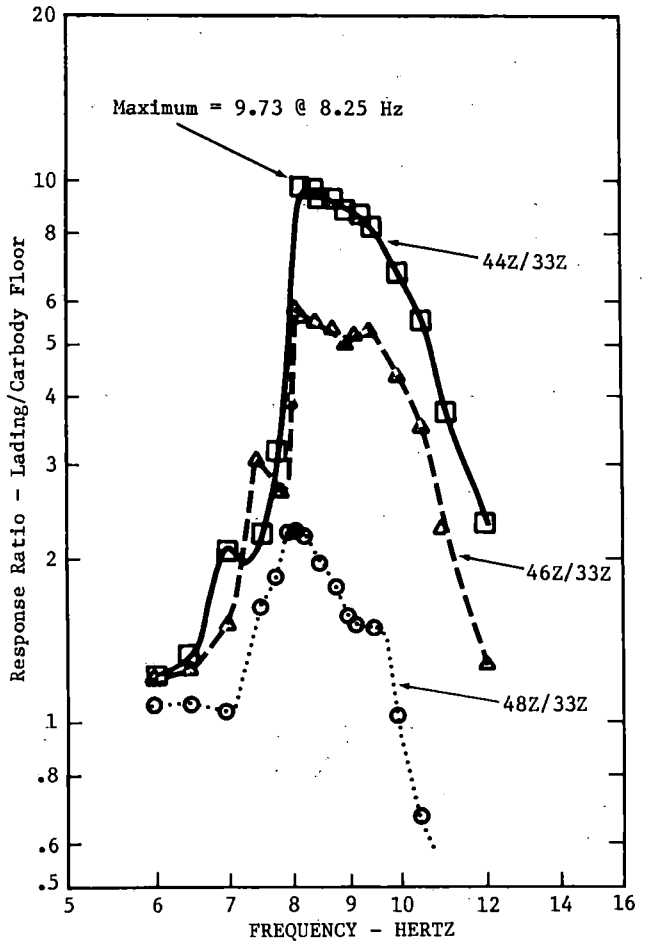


FIGURE 6.25 FREQUENCY RESPONSE, LADING VERTICAL MOTION, CONFIGURATION 3, B END

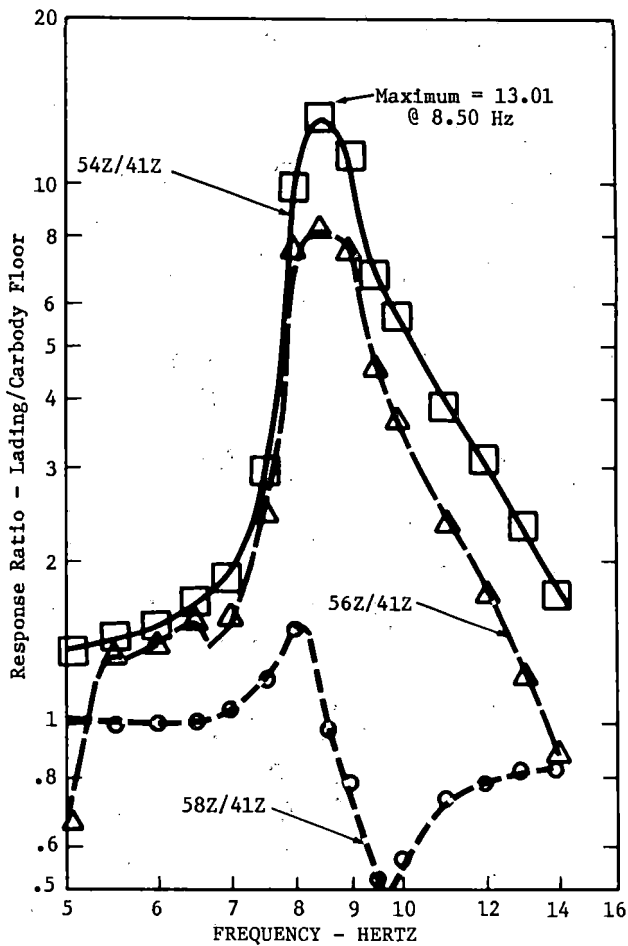


FIGURE 6.26 FREQUENCY RESPONSE, LADING VERTICAL MOTION, CONFIGURATION 1A, A END

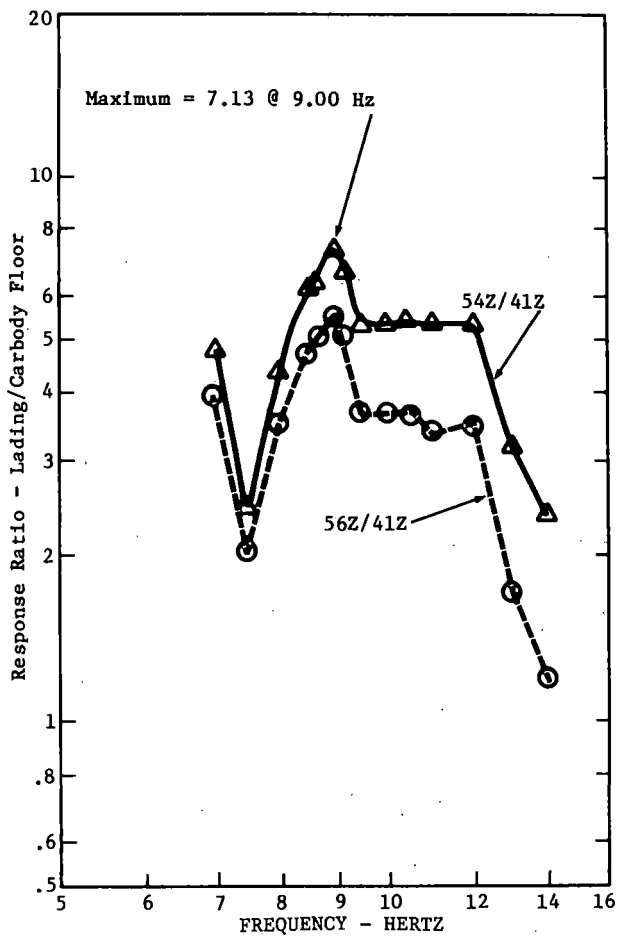


FIGURE 6.27 FREQUENCY RESPONSE, LADING VERTICAL MOTION, CONFIGURATION 1B, A END

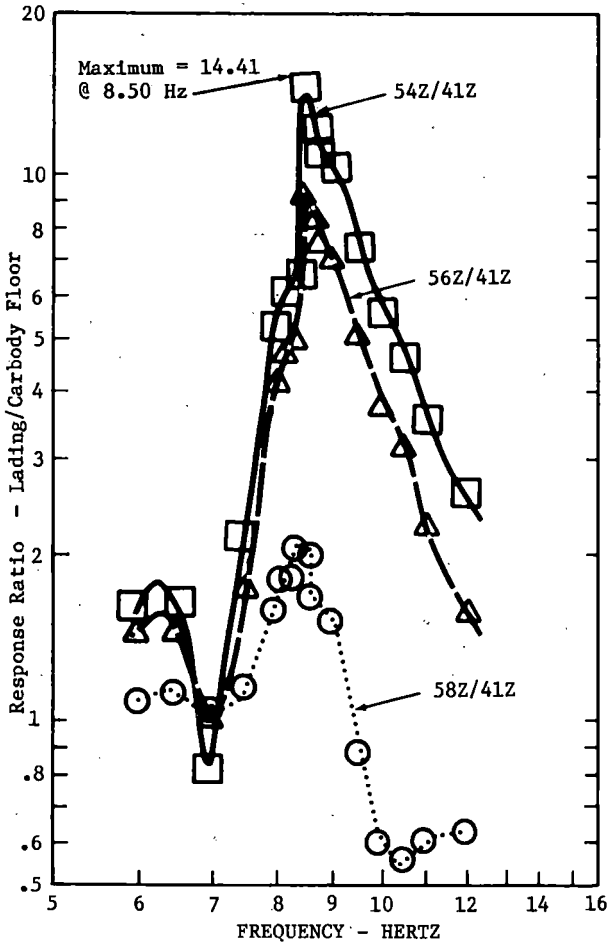
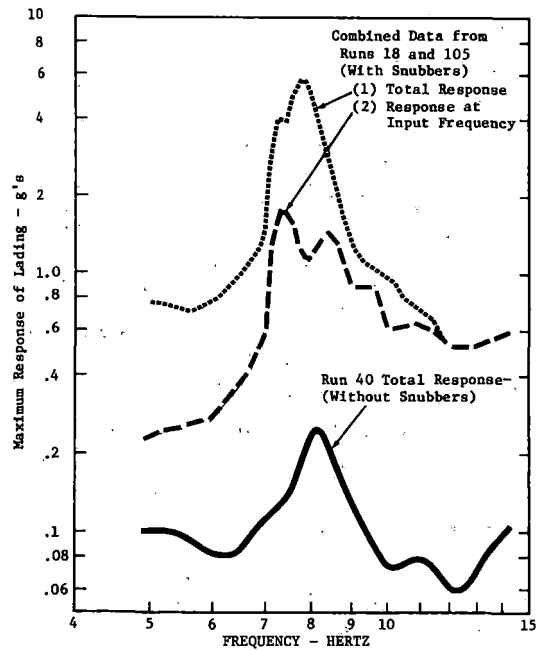


FIGURE 6.28 FREQUENCY RESPONSE, LADING VERTICAL MOTION, CONFIGURATION 3, A END

A suggested linear model of the lading vertical mode would be 8.6 Hertz with $Q=14$ for the pallet and stack configuration tested.

An initial comparison of lading acceleration responses in the oscillograph data showed that Runs 18 and 105 were very similar to each other and different from Run 40. The similarities were in the harmonics superimposed on the input frequency and the amplitude of lading response. Lading response in Run 40 was different in that it had a very clean sine wave at the input frequency and the amplitude of response was low in comparison. The data are summarized in Figure 6.29. Lading response from Runs 18 and 105 are combined, by enveloping, into two curves; one for the response at the input frequency and the other for the total response, i.e., the combined total of fundamental and harmonics. For Run 40 the total response is also the response at the input frequency. The lading accelerations with snubbers are seen to be 23 times greater than without friction snubbers. That is, the friction snubbers cause a much harsher ride within the frequency range of the lading vertical resonance.

An observation should be made on the degree of similarity of the lading responses for the corrugated boxes, Run 18 and the stretch wrap packaging, Run 105. Lading resonance modes are not sharply defined. They are affected by such things as the pallet condition and properties, the package stacking arrangement, the degree of slip between packages and the point at which package separation occurs. What was found in these tests was that the variation between packaging was less than the variation between different locations within the boxcar for the same packaging configuration.



Vertical Sinusoidal Motion Input of + 0.30 g at Wheel-Rail Interface. Data from Oscillograph Records

FIGURE 6.29 COMPARISON OF LADING VERTICAL RESPONSE WITH AND WITHOUT FRICTION SNUBBERS

6.9 Response to Staggered Rail Simulation

The low joint profile characteristic of staggered joint bolted rail was simulated by a rectified sine wave form as specified in Reference 6. This was accomplished by imposing the rectified sine motion vertically at each wheel with time delays to produce 90° phase difference between right and left wheels and to reproduce the fore and aft time delays that are dependent on axle spacing, truck spacing, rail length and track speed. The amplitude of the rectified sine input to the wheels was controlled using the shaker piston displacement transducers in a feed back loop with the computer driven shaker control systems.

Accelerometers mounted on each wheel were used to measure the actual wheel motion for recording and analysis of test data. As it turned out, the impulse acceleration due to the low joint cusp simulation was 40-50 times the basic sine wave acceleration so that the only information obtained from the wheel accelerometers was due to wheel shock. In the analysis of carbody response data it was assumed that the amplitude of the rectified sine input motion was at the specified test level.

The acceleration shocks experienced by the wheels at the simulated rail joints are summarized in Figure 6.30. Despite the scatter of data the "g" levels are seen to vary linearly with track speed. The recorded "g" levels are probably lower than actual for two reasons: firstly the actual joints will have some rail end misalignment and gapping that will increase the severity of the shock, and secondly the test data was recorded after going through a 35 Hertz low pass filter. The duration of the wheel shock pulses as indicated by the data processing system was about .025 seconds, which is also the filter characteristic. If the shock pulses were actually shorter than the filter characteristic, for example, .010 seconds, the filter would have attenuated the magnitude and registered a pulse width characteristic of the filter. There is consequently the strong probability that the wheel shocks are of higher "g" level than recorded but there is no way of deducing the actual unattenuated "g" level. Figure 6.30 is presented as a lower limit of wheel shocks due to rail joints.

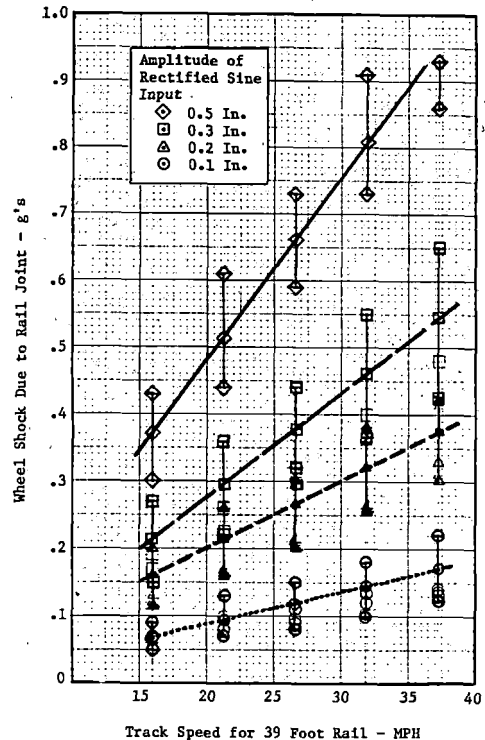


FIGURE 6.30 STAGGERED RAIL TEST. SHOCK IMPULSE AT WHEEL DUE TO RECTIFIED SINE CUSP AT SIMULATED RAIL JOINT

The primary reason for performing the staggered rail test was to measure the roll response of the carbody. The results are presented in plots of lateral response of the top of the carbody against the frequency of the input. (Note that the input frequency is defined as having a wave length equal to the rail length. The frequency of the functions used to generate the rectified sine wave is by definition half the input frequency. Note also that all amplitudes shown are single amplitude, noted as S.A.) In these plots the input frequency is shown at the bottom and the track speed is shown at the top using the relationship

$$f = v/\lambda$$

Where

- f = input frequency in Hertz
- = 2 x f (rec. sine)
- v = track speed in feet per second
- λ = rail length in feet,

assuming 39 foot rail, and converting frequency to miles per hour (MPH):

$$\text{MPH} = 26.591 \times f$$

The amplitude of the carbody roll response is given both as inches of lateral deflection at the top of the carbody and as carbody roll angle using the equation:

$$\phi = X/h \times 57.3$$

Where

- ϕ = carbody roll angle in degrees, S.A.
- X = amplitude of lateral motion at top of the carbody (measurements 31X, 37X and 39X) in inches, S.A.
- h = vertical distance of the measurement point from top of rail in inches.

This equation assumes that the roll motion of the carbody is about a center of rotation that is at the top of rail, as was found to be the case for the First Roll Mode in Section 6.1.

The data are plotted to show the effect of input level for each configuration tested, Figures 6.31 through 6.34, and to show a comparison between the configurations, Figures 6.35 through 6.37. For configurations with friction snubbers, the frequency (speed) of maximum roll angle is seen to vary significantly with input amplitude, Figures 6.31 and 6.34. In Configuration 1A the critical speed is seen to be 24, 21, and 18.6 MPH for input levels of 0.10, 0.20, and 0.30

inches respectively. These same numbers are also seen to occur for Configuration 3; however, the additional test at 0.50 inches showed the same critical speed as 0.30 inches (18.6 MPH).

Without snubbers, Configuration 1B (loaded) and 2 (empty), the roll frequency did not change when the input level was increased from 0.10 to 0.20 inches: 0.60 Hertz for the loaded condition (Figure 6.32) and 0.80 Hertz when empty (Figure 6.33). Because of the large response at 0.20 inches the Configuration 1B testing was discontinued. The Configuration 2 test at 0.30 inches indicates that the critical frequency is still at 0.80 Hertz but that when the roll motion reaches about 1.9 degrees, the linear range of the truck suspension system is exceeded and the nonlinear properties limit the response. The oscillograph data shows that, both in the 0.20 and 0.30 inch runs, nonlinear effects are evident when the carbody roll motion reaches 1.6 degrees.

There are two conclusions that can be drawn from comparing the effects of configuration changes in Figures 6.35, 6.36 and 6.37. The first is as expected, the friction snubbers reduce the magnitude of the carbody roll response by 60-70%. The second conclusion is that the lading package change from cardboard boxes to plastic stretch wrap had no measurable effect on the roll response of the carbody in the staggered rail rest.

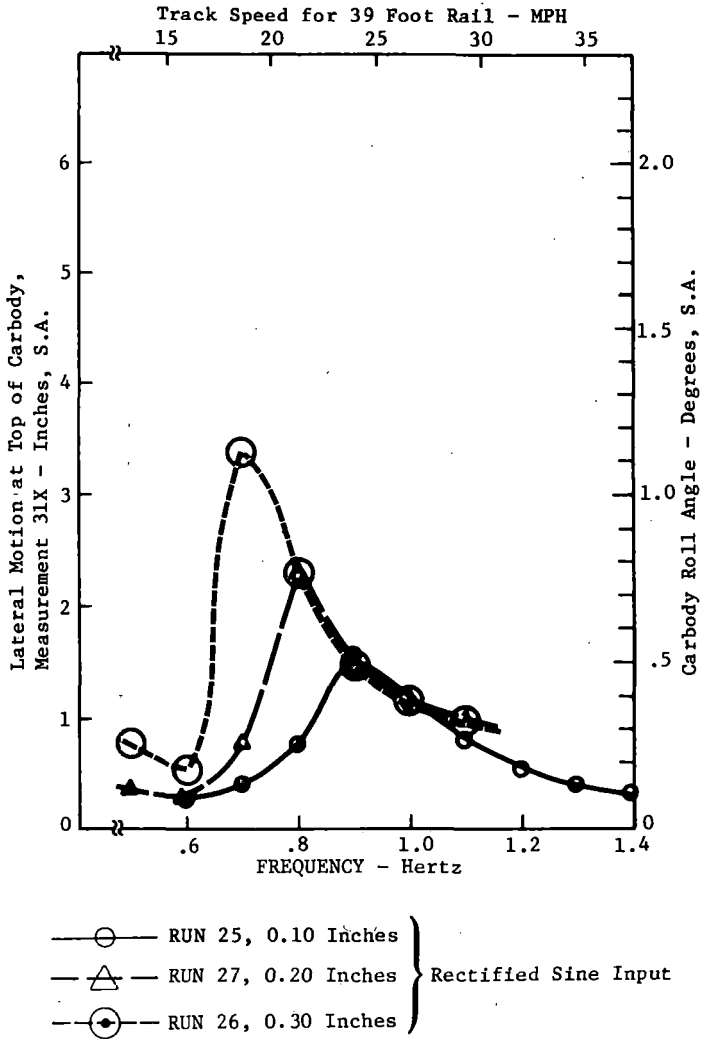


FIGURE 6.31 STAGGERED RAIL TEST, CONFIGURATION 1A EFFECT OF INPUT LEVEL

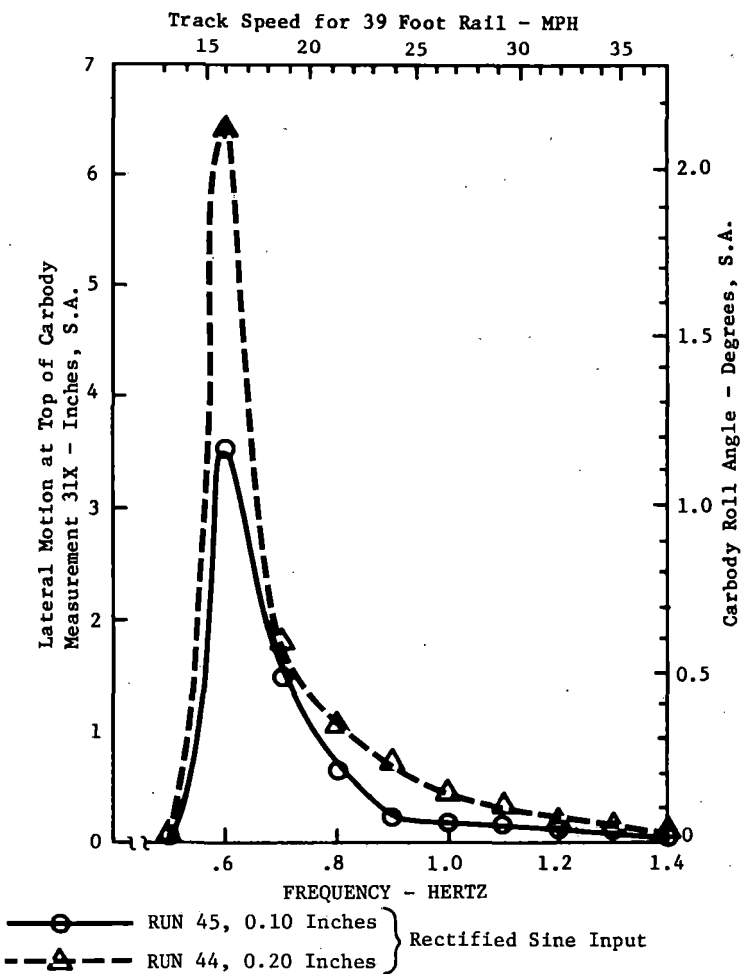


FIGURE 6.32 STAGGERED RAIL TEST, CONFIGURATION 1B, EFFECT OF INPUT LEVEL

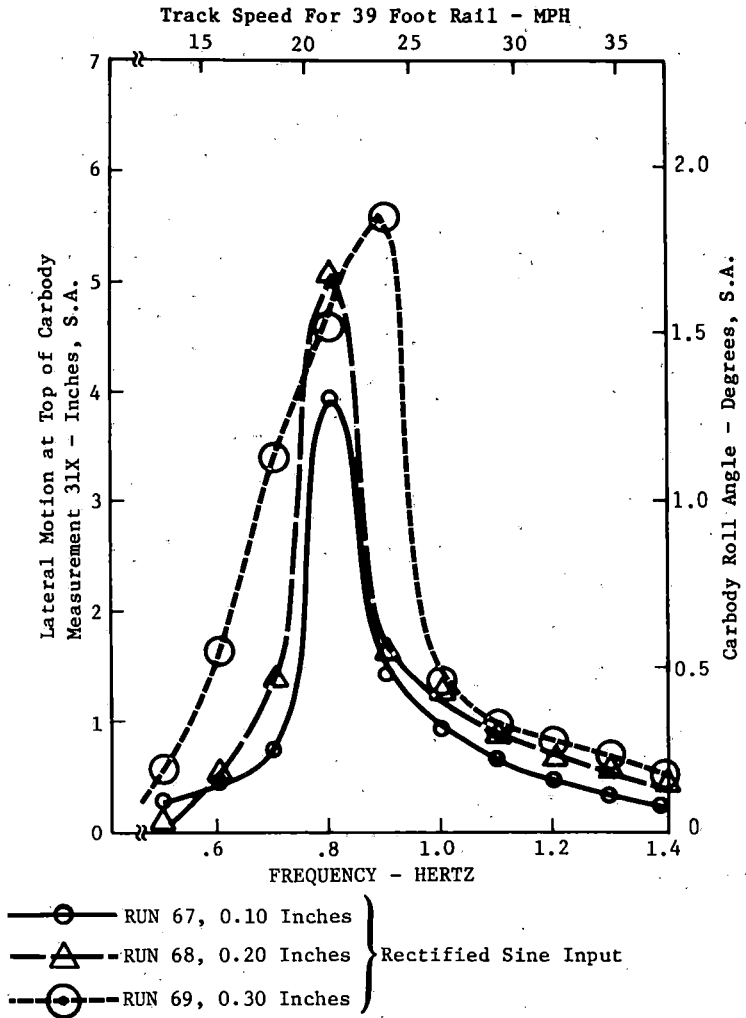


FIGURE 6.33 STAGGERED RAIL TEST, CONFIGURATION 2, EFFECT OF INPUT LEVEL

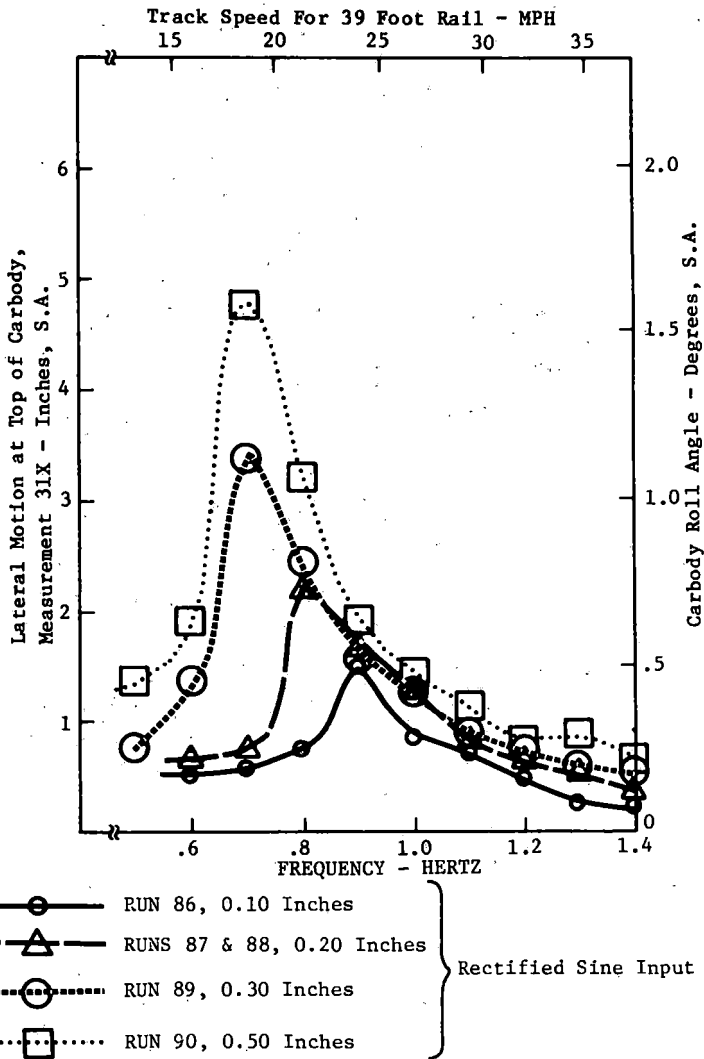
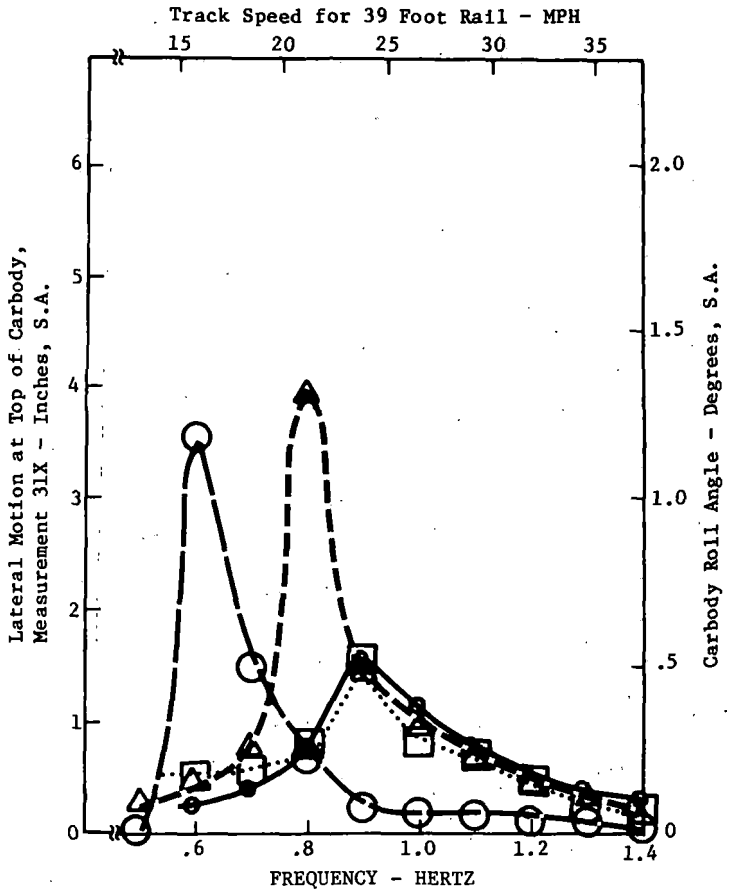


FIGURE 6.34 STAGGERED RAIL TEST, CONFIGURATION 3, EFFECT OF INPUT LEVEL



- RUN 25, CONFIGURATION 1A
- RUN 45, CONFIGURATION 1B
- △— RUN 67, CONFIGURATION 2
- RUN 86, CONFIGURATION 3

FIGURE 6.35 STAGGERED RAIL TEST-EFFECTS OF CONFIGURATION WITH 0.10 INCH RECTIFIED SINE INPUT

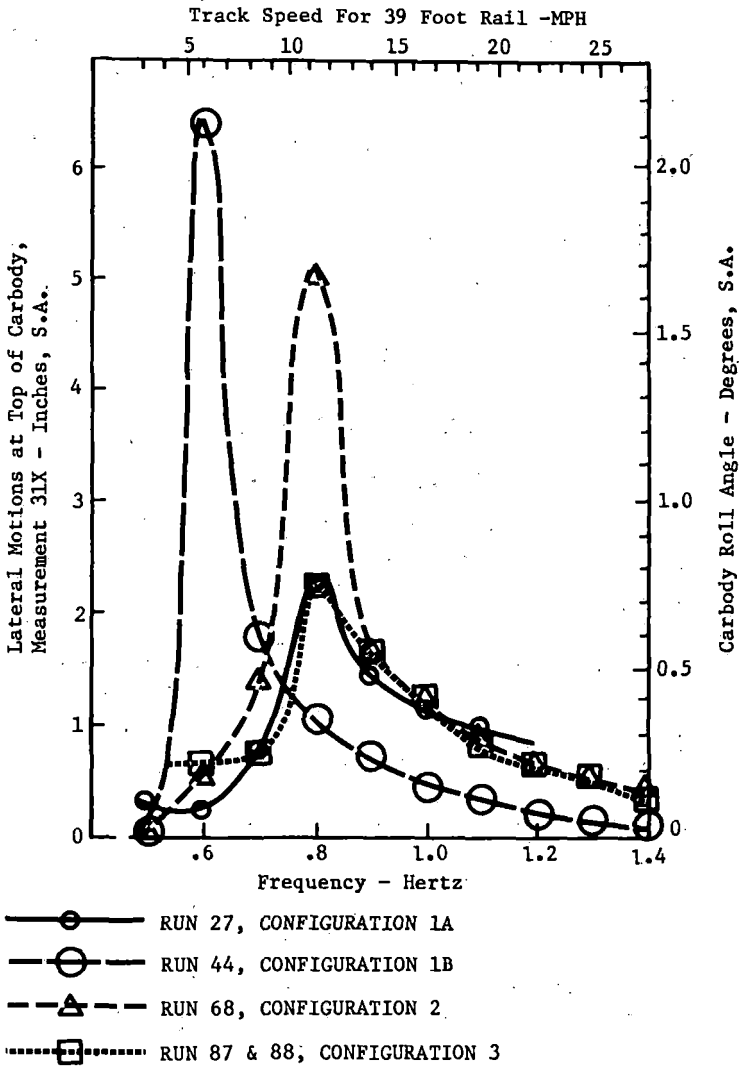


FIGURE 6.36 STAGGERED RAIL TEST-EFFECTS OF CONFIGURATION WITH 0.20 INCH RECTIFIED SINE INPUT

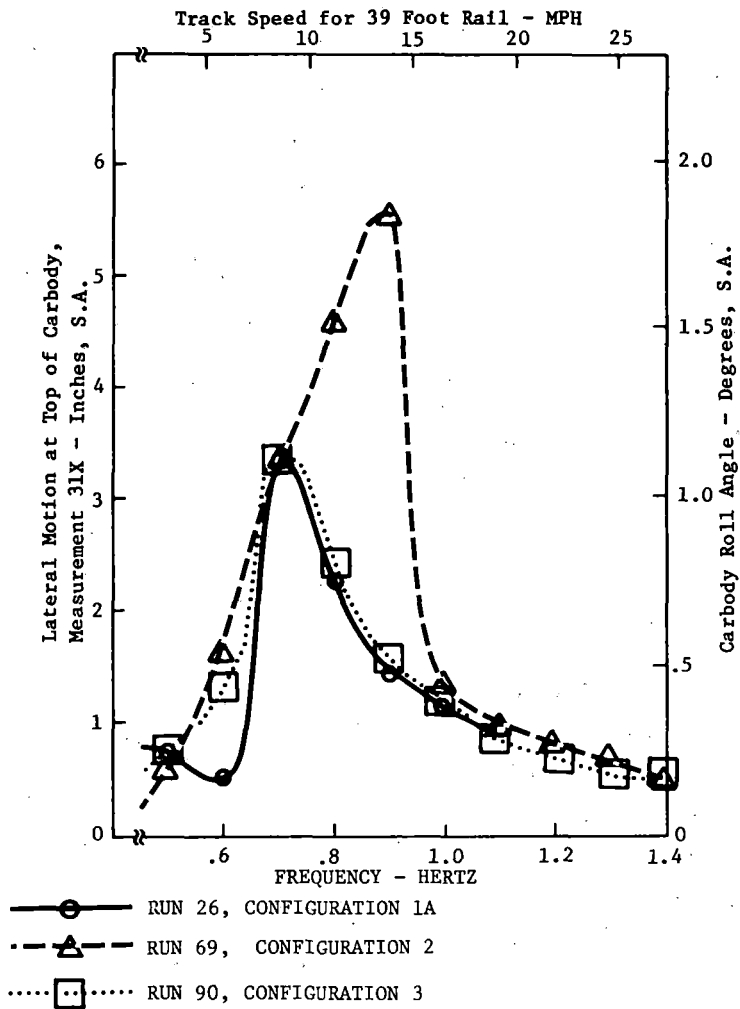


FIGURE 6.37 STAGGERED RAIL TEST-EFFECTS OF CONFIGURATION WITH 0.30 INCH RECTIFIED SINE INPUT

6.10 Hunting Simulation

The objective of the Hunting Simulation tests was to impose lateral motions on the trucks that would result in the truck lateral and carbody yaw motions characteristic of body hunting and to observe the responses of carbody and lading. These results were to be used in two ways: first to provide data on the response of carbody and lading during body hunting and second to provide a basis for demonstrating the accuracy of the FRATE model.

The four configurations tested are compared in Figure 6.38 for a yaw input of 0.20 inches (or equal to $\pm .047$ degrees of yaw motion). The two configurations with snubbers, 1A, with corrugated boxes and 3, with stretch wrap packaging, were also tested to input levels of 0.40 and 0.60 inches: response data is plotted in Figures 6.39 and 6.40. A summary of response ratios is given in Table 6.8.

Two general observations are made. First the friction snubbers are effective in suppressing carbody motions, at least to the 0.60 inch level tested. (This input amplitude corresponds to the hunting motion of a truck where rail gauge clearance is 1.2 inches.) The second observation is that the stretch wrap lading responds at slightly larger amplitudes than does the corrugated box.

Lading response data is also plotted in acceleration units of gravity ("g") in Figure 6.41 for input level of 0.20, 0.40, and 0.60 inches. In all cases there was bumping of the lading where the bumping was of two types: with large lateral motion of the lading the top of the stack bumped the side wall of the carbody and with one "g" vertical acceleration the top packages would bounce. This is easily recognized in the oscillograph traces; without bumping, the acceleration time history is a reasonably smooth sine wave. With bumping, there are high frequency transient vibrations in evidence, the magnitude of which is a measure of the severity of the bumping. Examples of time traces are shown in Figure 6.42.

The data plotted in Figure 6.41 shows that the "g" response of the lading package at the input frequency is essentially the same for both types of packaging. That the "g" levels can be equal even though the stretch wrap deflection amplitude is larger is possible because the maximum values for the stretch wrap occur at a lower frequency. The data shows that the high frequency "g" levels are about the same for both packagings but that maximum values are reached at different frequencies.

Finally it appears that in the hunting simulation, the lading, in either package, experiences severe and potentially damaging acceleration loadings.

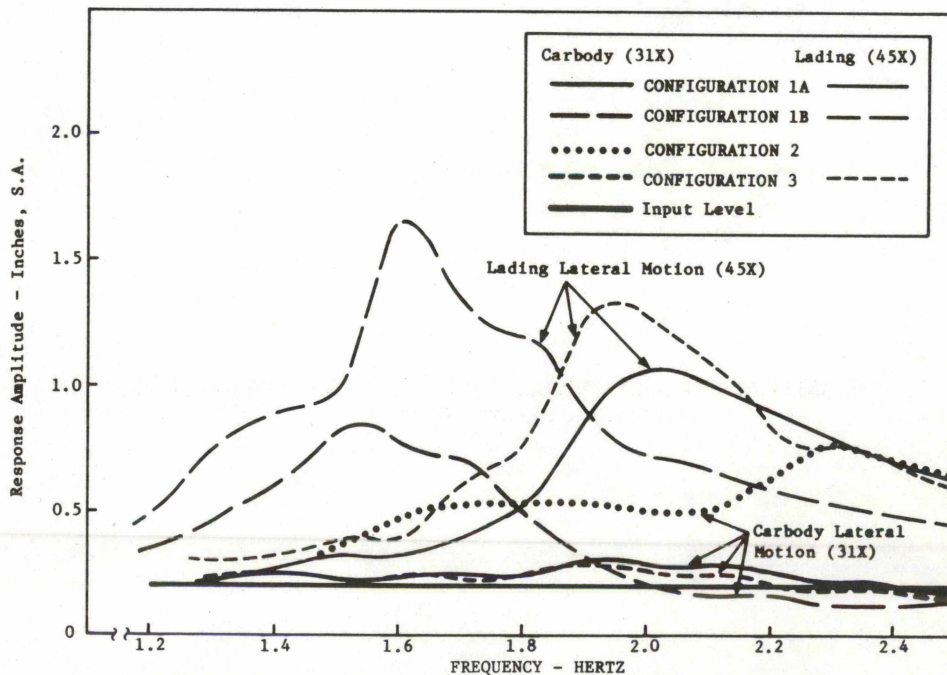


FIGURE 6.38 HUNTING SIMULATION TEST WITH 0.20 INCH ($\pm .047^\circ$) YAW INPUT. CARBODY AND LADING LATERAL MOTIONS COMPARED

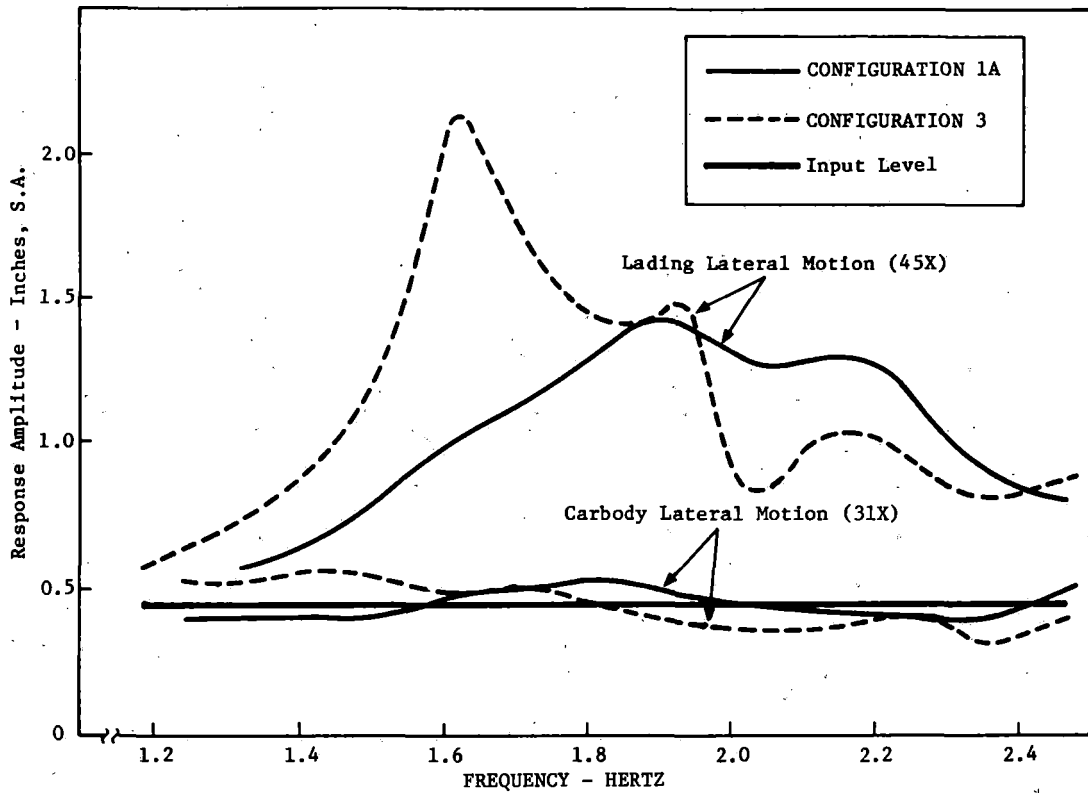


FIGURE 6.39 HUNTING SIMULATION TEST, RESPONSE TO 0.40 INCH ($\pm 0.094^\circ$) YAW INPUT. CARBODY AND LADING LATERAL MOTIONS COMPARED

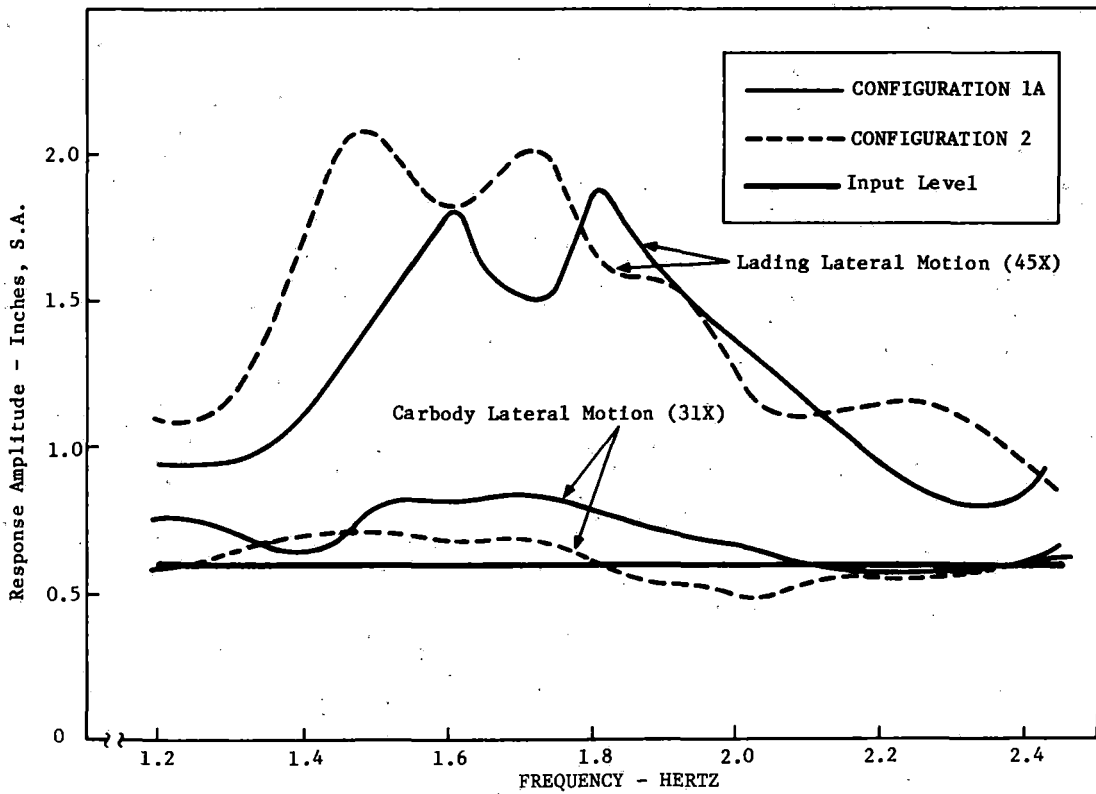


FIGURE 6.40 HUNTING SIMULATION TEST, RESPONSE TO 0.60 INCH ($\pm 0.14^\circ$) YAW INPUT. CARBODY AND LADING LATERAL MOTIONS COMPARED

TABLE 6-8 RESPONSE IN HUNTING SIMULATION

Measurement Location	Approximate Response Ratios			
	Without Snubbers		With Snubbers	
	0.2 In. Input	0.2 In. Input	0.4 In. Input	0.6 In. Input
Carbody (31X)	3.8	1.5	1.5	1.3
Corrugated Box (45X)	8.3	5.5	3.5	3.1
Stretch Wrap (45X)	--	8.0	5.3	3.5

NOTE: Response Ratios are Response/Input.

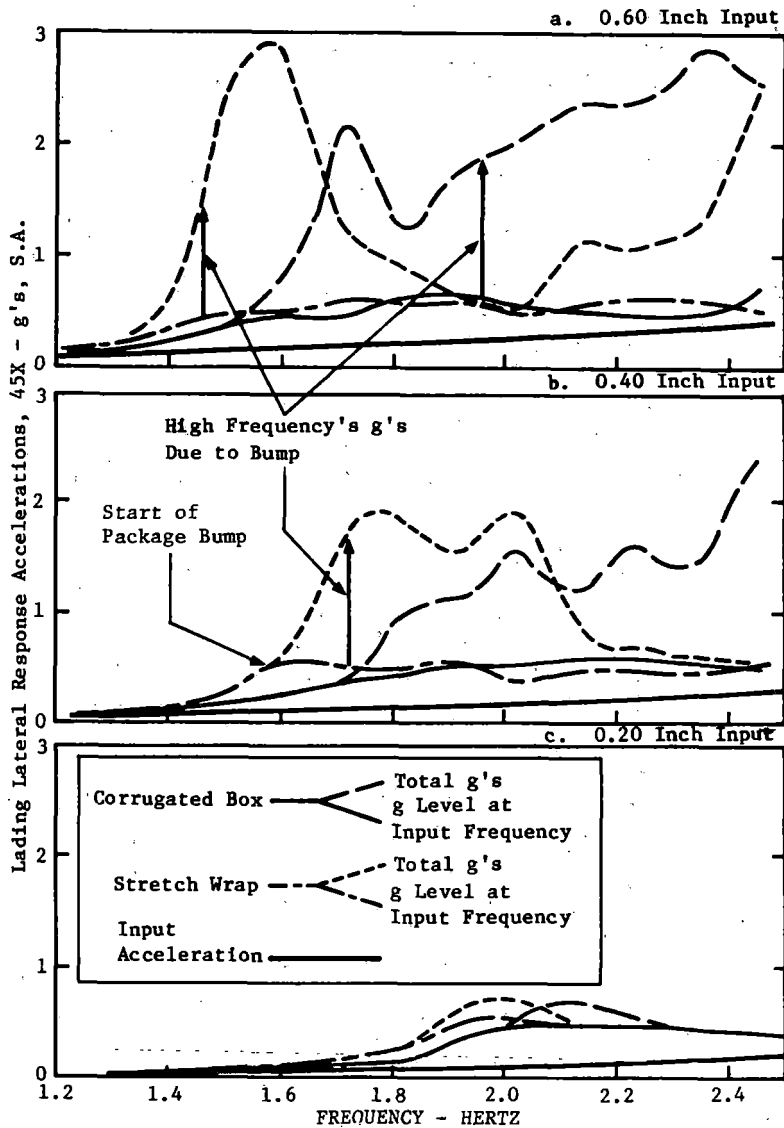


FIGURE 6.41 HUNTING SIMULATION, COMPARISON OF ACCELERATIONS IN LADING PACKAGING. MEASUREMENT NO. 45X

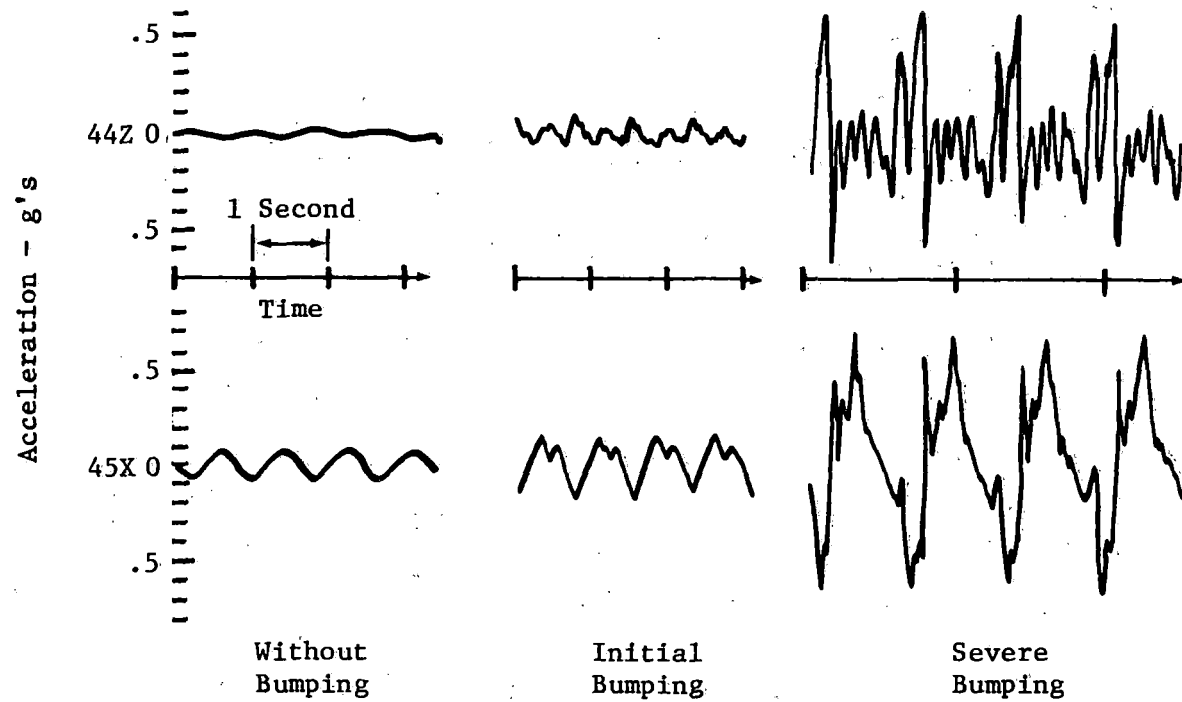


FIGURE 6.42 EXAMPLE TIME TRACES OF LADING ACCELERATIONS SHOWING CHARACTERISTIC WAVEFORM WITH AND WITHOUT BUMPING

6.11 Response to Vertical Bump Simulation

The increased stiffness of track and roadbed at railroad crossings is felt as a vertical bump in the track by traversing vehicles. The bump actually has two causal elements; one is the increased stiffness of the track-tie assemblage, the other is because the roadbed will have less settling at the railroad crossing. These bumps can be large enough to cause a vehicle to jump the track.

A vertical bump was simulated in the testing with a $(1-\cosine)/2$ function (haversine), with the length of the bump and the speed of the car tuned to the pitch mode of the test boxcar using the following relationship:

$$V = L f_p / 1.5$$

$$PL = .8V / f_p$$

Where

- V = car speed, feet per second
- f_p = pitch resonant frequency of the boxcar, Hertz
- PL = pulse length, feet
- L = truck spacing, feet

Thus, if we have:

$$\begin{aligned} f_p &= 2.9 \text{ Hertz and} \\ L &= 40.75 \text{ feet} \end{aligned}$$

we would use:

$$\begin{aligned} V &= 78.78 \text{ feet/sec (53.7} \\ &\text{mph) and} \\ PL &= 21.73 \text{ ft.} \end{aligned}$$

To tune for the bounce mode the equation would be:

$$V = Lf_b \text{ or } = Lf_b/2$$

Then with

$$\begin{aligned} f_b &= 2.2 \\ V &= 89.7 \text{ or } 44.8 \text{ ft/sec} \\ &= 61.1 \text{ or } 30 \text{ mph} \\ \text{and } PL &= 32.6 \text{ or } 16.3 \text{ feet} \end{aligned}$$

The shaker input for the testing was programmed to a bump duration and time delays between axles at and 10% above and below the boxcar pitch frequency. Problems were encountered in the shaker control software and the test was not performed for configuration 1A and only one successful run was made for configuration 1B. These results are shown in Figures 6.43 and 6.44. The response was not in the pitch mode (2.77 Hertz) as expected but was rather in the bounce mode of 2.05 Hertz.

Problems in the shaker computer control programming continued in the testing of Configuration 2 and again only one successful run was made. The results of this run are presented in the time history plots of Figure 6.45. The plots of vertical accelerations at both ends and center of the carbody show that both the bounce and pitch modes were present. The center of the carbody was moving at a steady 3.78 Hertz motion while the ends of the carbody were moving at 4.06 Hertz with a .274 Hertz amplitude modulation. Using the trigonometric formula:

$$\begin{aligned} \sin x + \sin y &= 2 \sin (1/2 (x + y)) * \\ &\cos 1/2 (x - y) \end{aligned}$$

and letting x = bounce frequency
and y = pitch frequency

then:

$$\begin{aligned} x &= 3.78 \text{ Hertz} \\ 1/2(x + y) &= 4.06 \text{ Hertz} \\ 1/2(x - y) &= .274 \text{ Hertz} \end{aligned}$$

from which $y = 4.33$ Hertz.

The input pulse duration was .271 seconds and the maximum carbody responses were +1.5 and -2.6g at 4.06 Hertz (this comes to up .89 and down 1.54 inches) at the truck location and +.95g at 3.78 Hertz (or \pm .65 inches) at the carbody center.

17

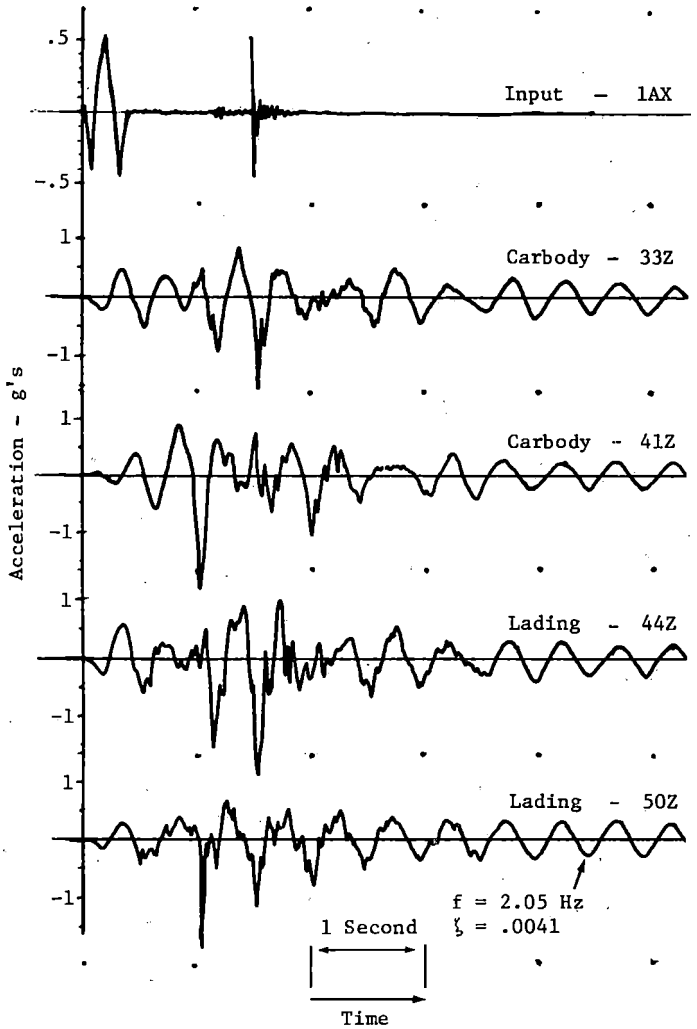


FIGURE 6.43 VERTICAL BUMP SIMULATION, CONFIGURATION 1B, VERTICAL RESPONSES

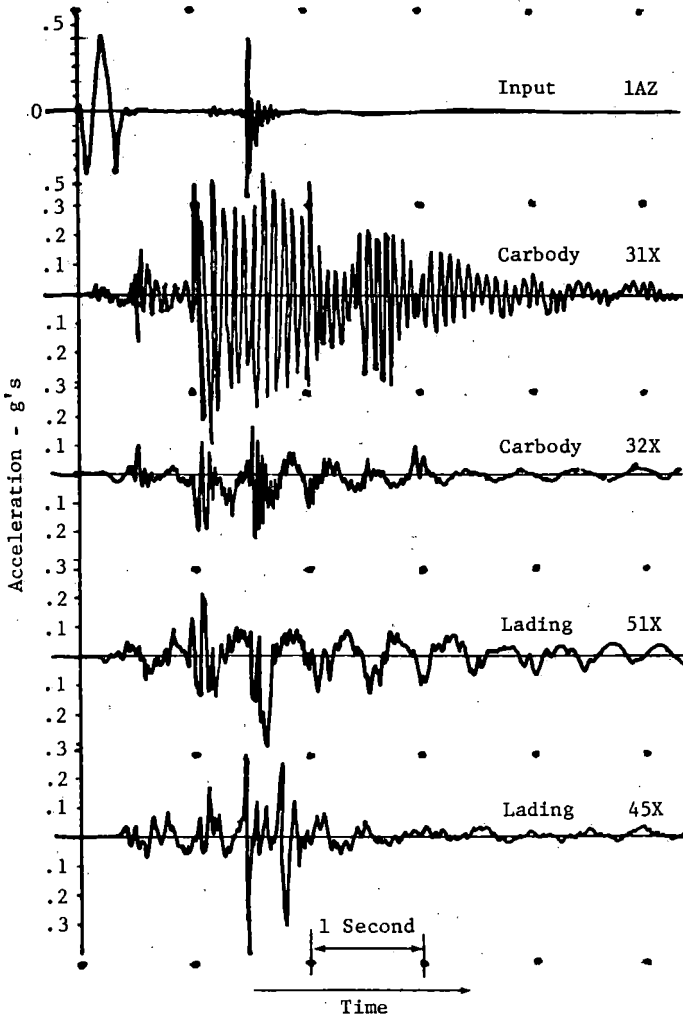


FIGURE 6.44 VERTICAL BUMP SIMULATION, CONFIGURATION 1B, LATERAL RESPONSES

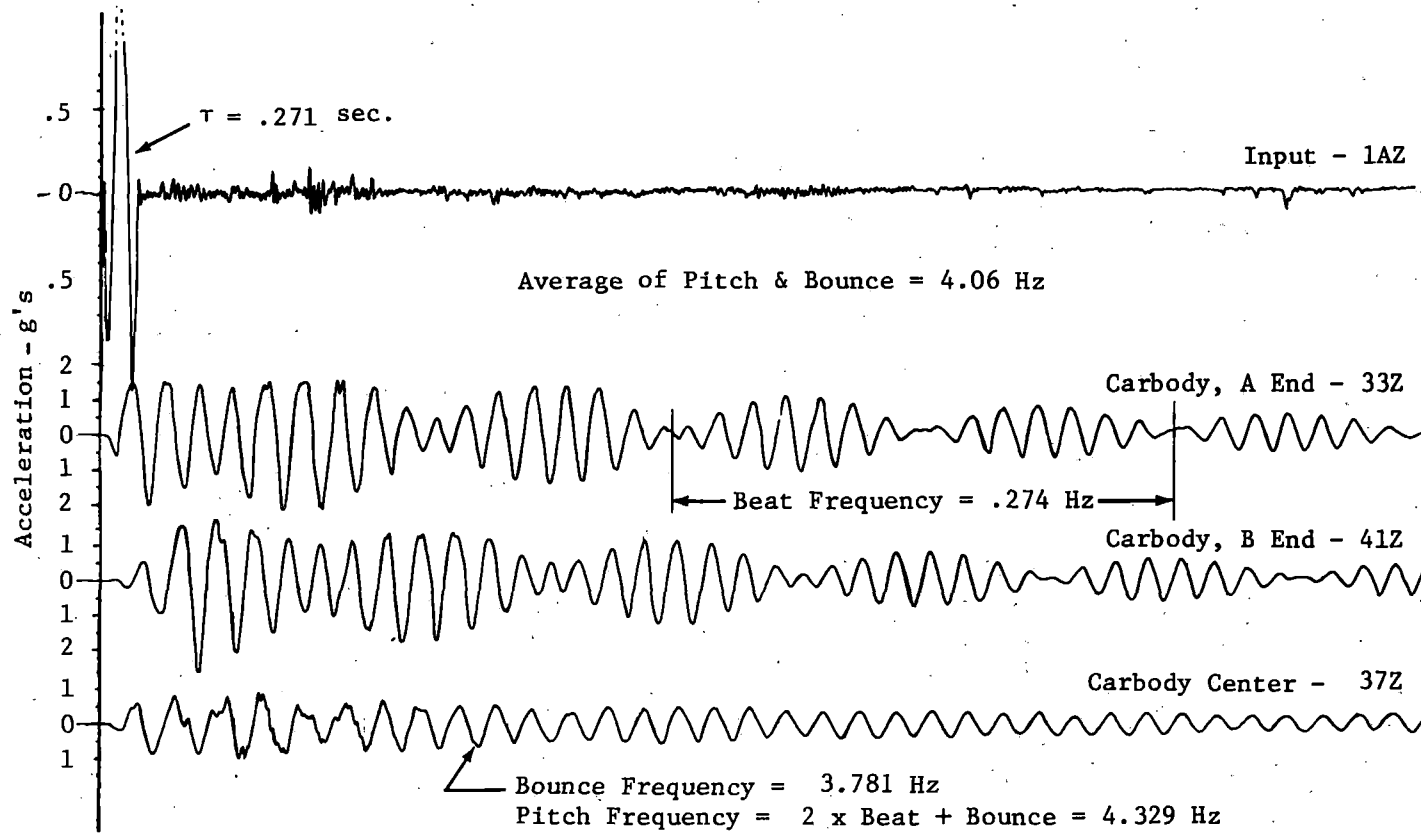


FIGURE 6.45 VERTICAL BUMP SIMULATION, CONFIGURATION 2

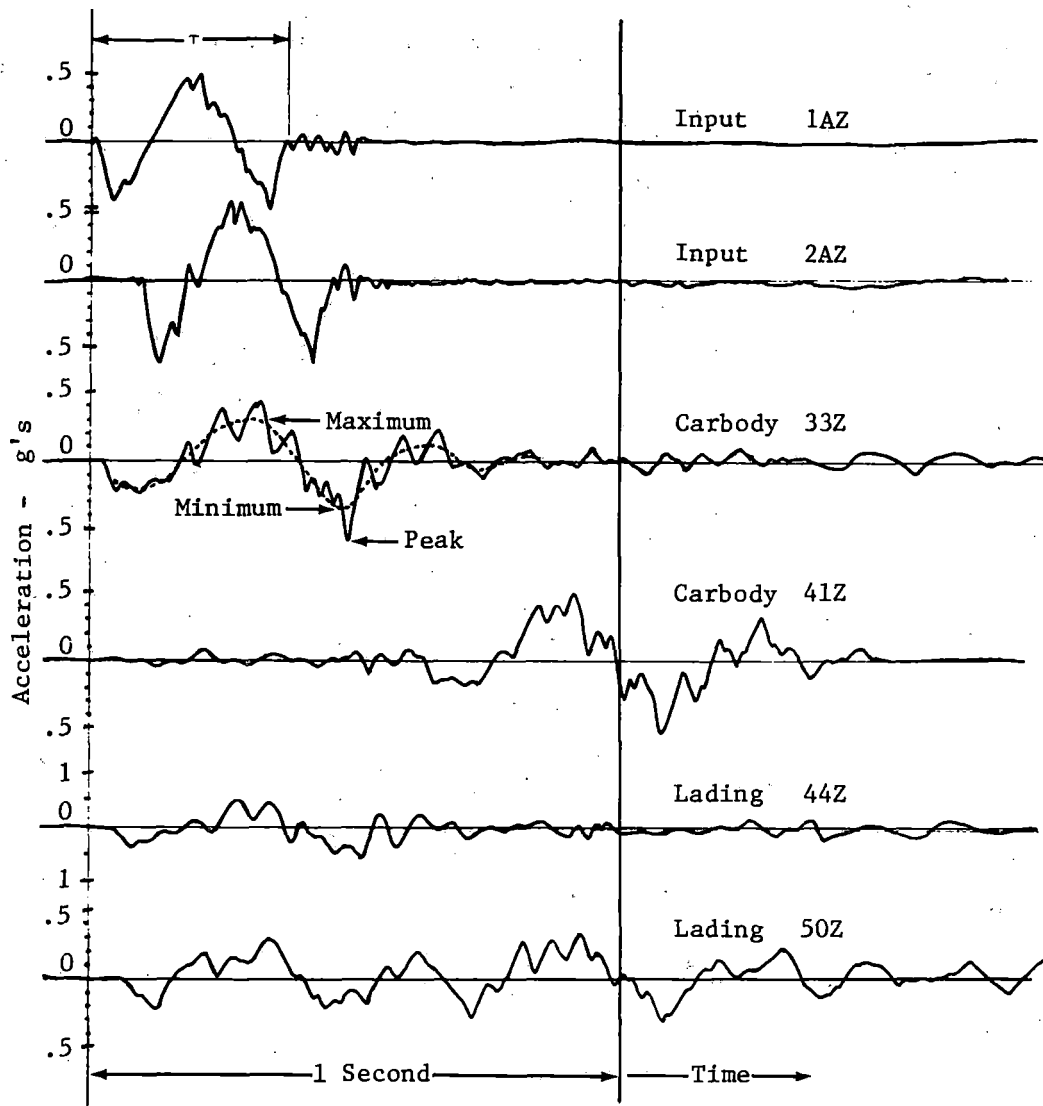


FIGURE 6.46 VERTICAL BUMP SIMULATION, CONFIGURATION 3

In Configuration 3 there were three runs made using a vertical track bump 1.0 inches high with three different pulse durations and speed simulations. The time history plots in Figures 6.46 are from the first run and are representative of all three. The boxcar response motions were very quickly damped out (in about one and a half cycles) and were in the 2.7 to 3.0 Hertz range which is within the frequency range of the pitch mode. A summary of results is given in Table 6.9.

The acceleration level of responses is seen to increase with the higher speed runs, but the slowest run is seen to have the largest Q (output/input ratio).

The responses for Configuration 3 are relatively small leading to the conclusion that with the strong snubbers the boxcar bounce and pitch motion are well controlled for the track bump characteristic of railroad crossings.

TABLE 6-9 TRACK IRREGULARITY TEST RESULTS--CONFIGURATION 3
(Units are Acceleration in g's Except as Noted Otherwise)

Measurement Item	Run 94			Run 95			Run 96		
	Max.	Min.	Peak	Max.	Min.	Peak	Max.	Min.	Peak
Input 1AZ	+ .48	- .40	.52	+ .70	- .60	+ .72	.88	- .87	.96
τ , Actual	.349 sec = 1/2.87 Hz			.303 sec = 1/3.30 Hz			.264 sec = 1/3.79 Hz		
τ , Desired	.400 sec = 1/2.50 Hz			.333 sec = 1/3.00 Hz			.294 sec = 1/3.40 Hz		
Carbody 33Z	+ .32	- .32 (2.87 Hz)	- .56	.42	- .44 (2.98 Hz)	- .70	.55	- .60 (2.91 Hz)	- .82
41Z	+ .36	- .24 (2.75 Hz)	.52	.44	- .46 (2.60 Hz)	- .70	.58	- .60 (2.85 Hz)	- .72
Lading 44Z	+ .30	- .35	+ .55	.50	- .41	- .75	.70	- .50	.95
50Z	+ .20	- .20	- .33	.26	- .20	- .32	.36	- .30	.54
Average Q	0.655			.60			.60		

Notes: See Figure 6.46 for definition of τ , Max., Min. and Peak. Numbers in Table are g's acceleration.

7. SUMMARY DISCUSSIONS

7.1 Modal Test Results

A summary of the modal frequencies obtained in each of the four configurations tested, as well as a set of FRATE analysis results is given in Table 7-1. There are 12 blanks in this 45 element matrix: the analytic prediction did not include body torsion and body bending; there are no lading modes in the empty configuration; the body bending mode was determined to be above 20 Hertz and out of the range of interest and planned testing; and, because of the overwhelming effects of the friction snubbers, there were three modes not found in Configuration 1A and one not found in Configuration 3.

Nevertheless, the modal testing was concluded to have been successfully completed. Complete sets of modes were obtained for Configurations 1B and 2 (loaded and empty with no snubbers) and these two are the primary cases needed to validate the FRATE program exclusive of the friction snubbers. The combined results of Configurations 1A and 3 are sufficient to define the properties and effects of the friction snubbers.

Comparison between the FRATE pre-test analysis and test results shows best comparison with Configuration 1B even though the FRATE analysis included a coulomb damping model of the friction snubbers. There are two reasons why the friction snubber modal may have

TABLE 7-1 MODAL FREQUENCY SUMMARY, 70 TON BOXCAR, HERTZ

CONFIGURATION DATA MODE	PREDICTION 57.5 Ton Snubbers Part Time	CONFIG 1A 60.1 Ton Snubbers In	CONFIG 1B 60.1 Ton Snubbers Out	CONFIG 2 Empty Snubbers Out	CONFIG 3 59.5 Ton Snubbers In
1st Roll	0.7	.69-.98	.54-.69	.84-1.00	.65-1.2
2nd Roll	1.6	N.A.	2.5-3.0	3.04	3.40-4.0
Yaw	1.7	N.A.	1.65-1.71	2.3-2.6	N.A.
Bounce	2.2	N.A.	2.05	3.81	2.1-2.8
Pitch	2.9	3.4-4.5	2.77	4.34	3.3-4.4
Body Torsion	--	12.4 & 14.1	13.67 & 15.36	13.125 & 14.75	13.17 & 14.8
Body Bending	--	Above 20.0	Above 20.0	Above 20.0	Above 20.0
Lading Lat.	3.0	1.7-2.8	1.65-1.71	--	1.60-2.4
Lading Vert.	9.0	8.5-8.7	9.00-9.25	--	8.25-8.5

NOTES:

N.A. - not available (snubbers remained locked)

Body Torsion - Two modes were found: (1) coupled with carbody yaw;
(2) uncoupled.

been insufficient: first, a 3,000 pound force value was used in the model whereas the test vehicle was measured to be about 5,400 pounds; second, the friction snubber was modeled in FRATE to be active only after side bearing contact. From the test results presented in Reference 1, this is not the case and the model needs to be modified to be active for any relative position of the carbody and dependent only on the force applied to the snubber. This is not a difficult change to make and will probably show a significant increase in the effectiveness of the snubbers in the FRATE program.

In the comparison of modal frequencies between FRATE predictions and Configuration 1B, the second roll mode is the only freight car mode that differs significantly: 1.6 Hertz from FRATE and 2.5-3.0 Hz from tests. Finding the cause of and corrective measures for this difference will be tasks for the validation effort. However, the existing close correlation of the other modes provides reassurance that it will

not be difficult to validate the FRATE program with the boxcar model.

The lateral lading mode ranged from 1.6 to 2.2 Hertz and was lower than the predicted 3 Hertz. The validation effort to be performed will review the basis for the 3 Hertz prediction, extrapolate the experimental data, Reference 5, and make necessary revisions to the prediction procedure for both lateral and vertical modes.

In most cases it was found that the modal frequencies varied with amplitude of input. The double figures given in Table 7.1 are the end points of these frequency ranges. These modal frequencies are further summarized in Figure 7.1 by showing the total frequency variation for each mode over all four configurations. Figure 7.1 is helpful in showing the extent of frequency overlap for the modes below 4.0 Hertz. Particular note should be made of the overlap in (1) the carbody yaw and lading lateral modes and (2) the carbody bounce and pitch modes.

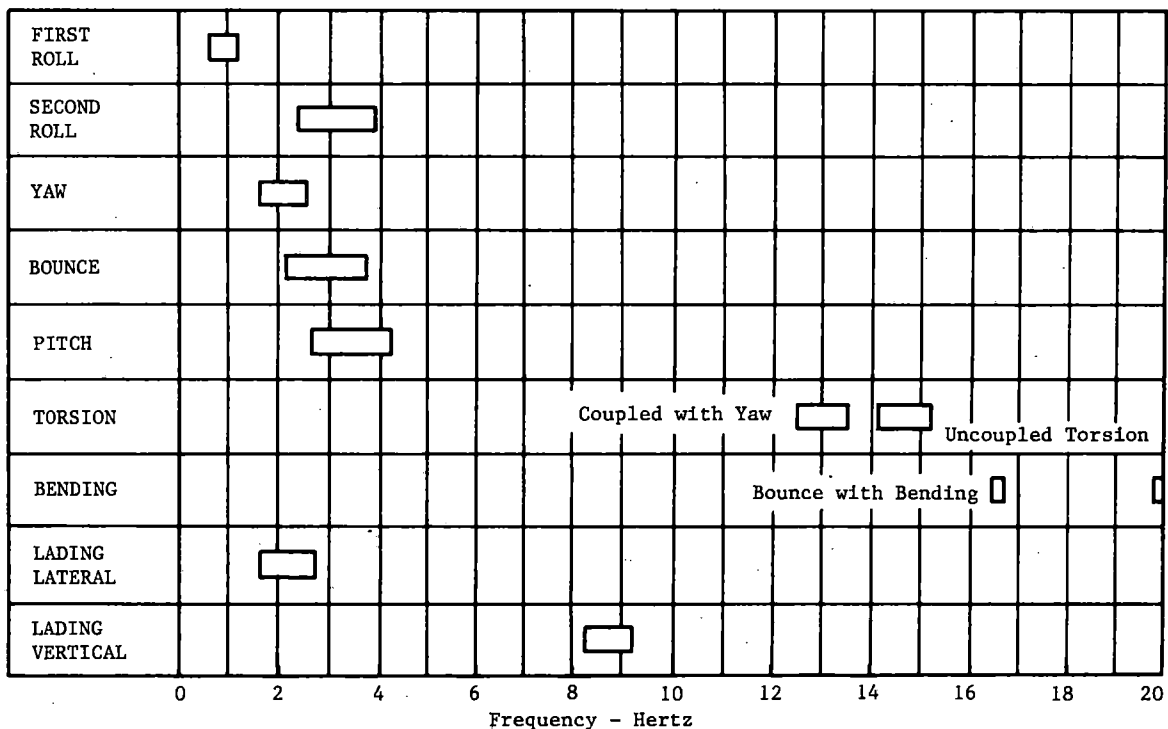


FIGURE 7.1 FREQUENCY RANGE OF EACH MODE FOR ALL CONFIGURATIONS

In studies of carbody hunting, the yaw inertia of the carbody should include the dynamic effects of the lading lateral mode. Conversely, in the study of lading environments, the lading dynamics coupled with hunting conditions should be included.

In the study of boxcar response to vertical transients, such as railroad crossings, the pitch and bounce must both be included in the dynamic analysis.

A final observation on the modal test results is on the strong influence of the friction snubbers. The snubbers in all cases made the modal frequencies more sensitive to amplitude. In most cases the snubbers caused the frequencies to be higher (second roll, pitch and bounce) but for some cases to be lower (first roll at the larger amplitude). The snubbers were so effective for carbody yaw motions that they remained locked and yaw modes were not obtainable.

7.2 Track Condition Simulation

The performance of the DOTX 503 Boxcar in the staggered joint rail was good in that roll responses were relatively small and there was no wheel lift. This performance is due partly to the center of gravity of the vehicle being lower than a typical fully loaded hi-cube boxcar (see Table 3-2), and partly to the high force characteristics of the friction snubbers. Even though there were no surprises in the test results, there are a number of observations of interest to be made.

The critical speed for carbody roll varied significantly with the amplitude of the cross level variation. For the three rectified sine levels of 0.10, 0.20 and 0.30 inches the critical speeds were 24, 21, and 18.6 mph for both Configurations 1A and 3. With no friction snubber the critical speed was constant at 16.0 mph loaded (Configuration 1B) and 21.3 mph empty (Configuration 2).

The response curves, speed versus carbody roll angle, were, for the most part, typical of a decreasing speed run: there is a gradual increase in roll angle as speed is decreased to a maximum and then a relatively abrupt decrease in roll angle. The one case that did not follow this pattern closely was the 0.30 inch test in the empty, no snubber configuration.

In this case the response curve was typical of a nonlinear condition that partially truncated the usual peaking curve. It is probable that this nonlinear character was caused by gib contact.

The hunting simulation resulted in carbody motions that were only slightly larger (42%) than the input motions due to the snubbers being stiff and remaining locked. However, the lading responses were relatively large (5.4 times larger than input displacement) to the point that severe impact shocks resulted, due primarily to the lading hitting the carbody sidewalls. Maximum acceleration measured on the lading was 2.9g.

Rail car trucks will normally move from side to side (hunt), within the limits permitted by gauge clearance, at a predictable frequency that is dependent on a number of truck, vehicle and track parameters but is primarily a function of speed. Typically, in the speed range from 0 to 60 mph, the hunting will vary from 0 to 2.0 Hertz. Ideally the truck will be stable throughout its operating speed range and induced hunting motions will die out quickly. However, each truck-vehicle-track combination has a critical speed where the hunting motion, once induced, is sustained. Further, when the hunting frequency is near a body mode (usually carbody yaw), the truck hunting motion and body yaw mode couple into a condition known as body hunting and which is generally more severe than truck hunting.

The test philosophy was to assume a condition of body hunting existed for the test vehicle, to generate the truck hunting motions that would occur, and then to measure the characteristics of the body motion.

The results of the hunting simulation test followed the pattern found in the yaw mode testing. The friction snubbers very effectively limited the yaw motions of the carbody so that a classic body hunting condition was not induced in those cases with snubbers. However, the lading lateral mode fell into the same frequency range (1.6-2.8 Hertz) and large lading responses did occur. In tests without snubbers large body yaw motions did result and test input levels were limited to 0.20 inches because of the severity of the carbody motions.

The conclusions drawn are that, with this lading configuration, the lateral lading mode will couple with truck hunting to produce a kind of body hunting condition. Further, with reduced snubber forces, more typical of an older and weaker set of friction snubbers, body hunting (if encountered) will be very severe with a lot of lading participation. Although derailment conditions are not indicated, accelerated wear and increased probability of damage to track, truck, carbody and lading will result.

The lading dynamics are dependent primarily on the pallet and the height of the stack. The test configuration is consequently fairly typical but as the stack height is increased above the seven foot stack used, and as the total lading weight is increased, the hunting response conditions can be expected to worsen.

The tests simulating track irregularities typified by railroad crossings were successfully completed despite some computer programming problems for the shaker input control. The results showed that both the pitch and bounce modes can be excited by the track bump produced by typical track modulus changes. With snubbers, the response motions are controlled and damp out quickly. Without snubbers, the response motions are large, nearly 2 g's, for both the loaded and empty conditions and the bounce and pitch motions continue for many cycles.

8. CONCLUSIONS

The total test program including the static tests reported in Reference 1 and the vibration tests of this report are concluded to be successfully completed. The stiffness, damping, modal and response data obtained and reported are extensive and will be extremely valuable and helpful for the dynamic modeling and analysis of freight cars.

Comparison of the results of the existing FRATE boxcar model with test results shows, for the most part, very close agreement. The changes indicated by both the static and vibration testing are expected to be easy to do and the final validation of FRATE for boxcar dynamic analysis is not expected to be troublesome.

Lading, when loaded in typical pallet stacks, was shown to have a significant influence on the response of the boxcar in the harmonic roll responses to staggered rail and in hunting conditions. Loading configurations that result in minimum voids and the filling of voids with durable dunnage are recommended. Also the use of a more rigid pallet is recommended.

REFERENCES

1. Kachadourian, G., Summary Results of 70 Ton Boxcar Testing; DOT/ FRA/ ORD-82/23, The MITRE Corporation, April 1982.
2. Kachadourian G., Validation of FRATE for Boxcars, DOT/FRA/ORD-(to be issued).
3. Wilson, Nicholas G., 70 Ton Boxcar and Lading Test and Data Analysis Report, Boeing Services International, Inc., December 23, 1981.
4. Kachadourian, G. and N.E. Sussman, Validation of FRATE, Freight Car Response Analysis and Test Evaluation, MTR-8007, The MITRE Corporation, McLean, VA, December 1978.
5. Kachadourian, G., User's Manual for FRATX1 and FRATF1 Freight Car Dynamic Analysis Computer Programs FRA/ ORD-81-54, The MITRE Corporation, McLean, VA, July 1981.
6. Kachadourian, G., Vibration Test Requirements for a 70 Ton Boxcar-Revision 1, FRA/ORD-81-55, The MITRE Corporation, McLean, VA, July 1981.
7. Dorland, W.D. et al, Implementation Plan, Rail Dynamics Laboratory, Vibration Test Unit, 70 Ton Boxcar and Lading Test Program, VTU-IP-81-02-01, April 1981.

APPENDIX A
Measurements Numbering and Location

TABLE A-1 MEASUREMENT NUMBER AND DESCRIPTION

NUMBER	MEASUREMENT DESCRIPTION
(1Z) A1AZ	Input Accel, Vertical Actuator 1A, Left Side
(2Z) A1BZ	Input Accel, Vertical Actuator 1B, Right Side
(3X) A1CX	Input Accel, Lateral Actuator 1C
(4Z) A2AZ	Input Accel, Vertical Actuator 2A, Left Side
(5Z) A2BZ	Input Accel, Vertical Actuator 2B, Right Side
(6X) A2CX	Input Accel, Lateral Actuator 2C
(7Z) A3AZ	Input Accel, Vertical Actuator 3A, Left Side
(8Z) A3BZ	Input Accel, Vertical Actuator 3B, Right Side
(9X) A3CX	Input Accel, Lateral Actuator 3C
(10Z) A4AZ	Input Accel, Vertical Actuator 4A Left Side
(11Z) A4BZ	Input Accel, Vertical Actuator 4B, Right Side
(12X) A4CX	Input Accel, Lateral Actuator 4C
A13Z	Vertical Accel, B Truck, Left Sideframe
A14X	Lateral Accel, B Truck, Left Sideframe
A15Z	Vertical Accel, B Truck, Left End of Truck Bolster
A16X	Lateral Accel, B Truck, Left End of Truck Bolster
A17Z	Vertical Accel, B Truck, Right Sideframe
A18Z	Vertical Accel, B Truck Bolster, Right Side
A19Y	Longitudinal Accel, B Truck Bolster Center
D20Z	Vertical Displacement, B Truck, Left Side, Sideframe to Truck Bolster
D21Z	Vertical Displacement, B Truck, Right Side, Sideframe to Truck Bolster
A22Z	Vertical Accel, A Truck Left Sideframe
A23X	Lateral Accel, A Truck Left Sideframe
A24Z	Vertical Accel, A Truck Bolster, Left End

NOTES:

- (1.) Input accelerometers have two (2) sets of notations which are used interchangeably.
- (2.) Except for the input accelerometer notation in parentheses, the first letter refers to the instrument type (A = accelerometer, D = displacement and G = gyro), and the last letter, (X, Y, Z, & R) refers to the sensitive axis of the instrument--(R = roll).

APPENDIX A
Measurements Numbering and Location

TABLE A-1 MEASUREMENT NUMBER AND DESCRIPTION (Continued)

A25X	Lateral Accel, A Truck Bolster, Left End
A26Z	Vertical Accel, A Truck, Right Sideframe
A27Z	Vertical Accel, A Truck Bolster, Right End
A28Y	Longitudinal Accel, A Truck Bolster, Center
D29Z	Vertical Displacement, A Truck, Left Side Sideframe to Truck Bolster
D30Z	Vertical Displacement, A Truck, Right Side, Sideframe to Truck Bolster
A31X	Lateral Accel, Top, Left Side of Carbody, @ B Truck Center Line
A32X	Lateral Accel, Bottom, Left side of Carbody, @ B Truck Center Line
A33Z	Vertical Accel, Bottom, Left Side, of Carbody, @ B Truck Center Line
A34Z	Vertical Accel, Bottom, Right Side of Carbody, @ B Truck Center Line
A35X	Lateral Accel, Top, Left Side of Carbody, @ Carbody Center
A36X	Lateral Accel, Bottom, Left Side of Carbody, @ Carbody Center
A37Z	Vertical Accel, Bottom, Left Side of Carbody @ Carbody Center
A38Z	Vertical Accel, Bottom, Right Side of Carbody, @ Carbody Center
A39X	Lateral Accel, Top, Left Side of Carbody, @ A Truck Center Line
A40X	Lateral Accel, Bottom, Left Side of Carbody, @ A Truck Center Line
A41Z	Vertical Accel, Bottom, Left Side of Carbody, @ A Truck Center Line
A42Z	Vertical Accel, Bottom, Right Side of Carbody, @ A Truck Center Line
A43Z	Vertical Accel, Top of Lading, Right Side B Truck Center Line
A44Z	Vertical Accel, Top of Lading, Left Side @ B Truck Center Line
A45X	Lateral Accel, Top of Lading, Left Side @ B Truck Center Line
A46Z	Vertical Accel, Bottom of Top Pallet of Lading, Left Side @ B Truck Center Line

APPENDIX A
Measurements Numbering and Location

TABLE A-1 MEASUREMENT NUMBER AND DESCRIPTION (Concluded)

A47X	Lateral Accel, Bottom of Top Pallet of Lading, Left Side @ B Truck Center Line
A48Z	Vertical Accel, Bottom of Bottom Pallet of Lading, Left Side @ B Truck Center Line
A49Z	Vertical Accel, Inside Bottom of Lower Pallet of Lading, @ B Truck Center Line
A50Z	Vertical Accel, Top of Lading, Left Side, @ Carbody Center
A51X	Lateral Accel, Top of Lading, Left Side, @ Carbody Center Line
A52Z	Vertical Accel, Bottom of Lower Pallet of Lading, Left Side, @ Carbody Center Line
A53Z	Vertical Accel, Top of Lading, Right Side, @ A Truck Center Line
A54Z	Vertical Accel, Top of Lading, Left Side, @ A Truck Center Line
A55X	Lateral Accel, Top of Lading, Left Side, @ A Truck Center Line
A56Z	Vertical Accel, Bottom of Top Pallet of Lading, Left Side, @ A Truck Center Line
A57X	Lateral Accel, Bottom of Top Pallet of Lading, Left Side, @ A Truck Center Line
A58Z	Vertical Accel, Bottom of Lower Pallet of Lading, Left Side, @ A Truck Center Line
GAR	Roll Gyro, Mounted on Carbody Structure Six (6) Inches Above Draft Pocket, Car Center Line, A End
GBR	Roll Gyro, Mounted on Carbody Structure Six (6) Inches Above Draft Pocket, Car Center Line, B End

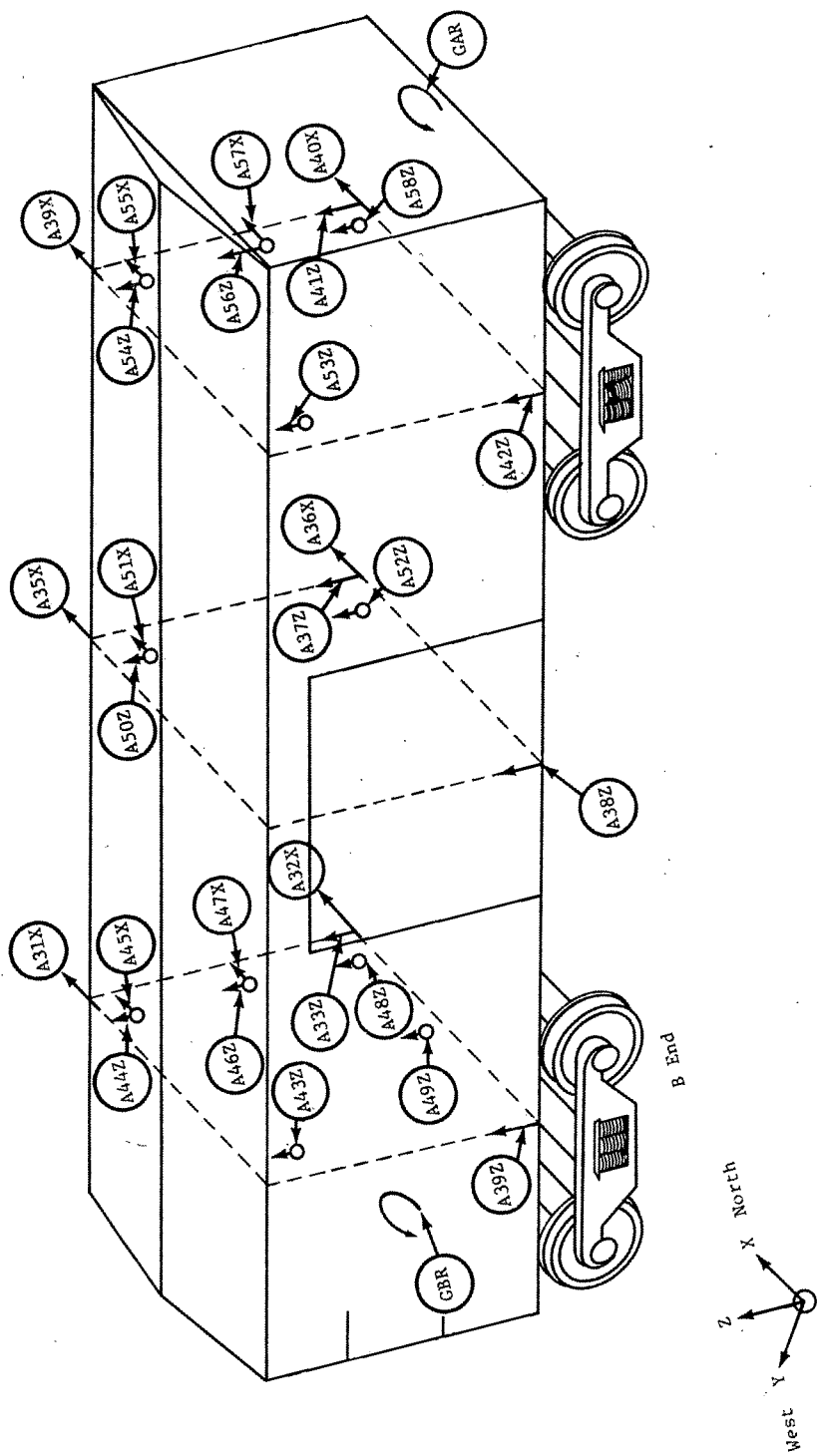


FIGURE A.1 MEASUREMENT LOCATION ON CARBODY AND

LADING—70 TON BOXCAR

Data Analysis Results of 70 Ton Boxcar
Vibration Tests, 1983
US DOT, FRA, George Kachadourian

Results of 70 Ton Boxcar
Vibration Tests, 1983
US DOT, FRA, George Kachadourian

SMEAD00VP53SA

PROPERTY OF FRA
RESEARCH & DEVELOPMENT
LIBRARY